498 | Oktober 1989

SCHRIFTENREIHE SCHIFFBAU

Harald Böttcher

Simulation of Ship Motions in a Seaway

TUHH
Technische Universität Hamburg-Harburg

Simulation of Ship Motions in a Seaway

Harald Böttcher, Hamburg, Technische Universität Hamburg-Harburg, 1989

ISBN: 3-89220-498-5

Schriftenreihe Schiffbau
Schwarzenbergstraße 95c
D-21073 Hamburg

http://www.tuhh.de/vss

INSTITUT FÜR SCHIFFBAU DER UNIVERSITÄT HAMBURG
Bericht Nr. 498

Simulation of Ship Motions in a Seaway

von

Harald Böttcher

Oktober 1989

Abstract

A method for simulating large amplitude ship motions in a seaway in six degrees of freedom is presented. Rigid body motion equations suitable for large motion amplitudes are derived. The simulation model takes into account all significant forces acting on a ship. Froude-Krilov forces and moments are calculated using the actual waterline along the hull. Hydrodynamic radiation and diffraction forces are calculated using higher-order differential equations relating the relative motion between the water and the ship sections to the section forces. The hydrodynamic coefficients are calculated using a linearised method, but at every time step the values corresponding to the instantaneous submerged shape of the ship are used. Other than in linearised calculations the coefficients of the equations of motion are independent of frequency. Thus the simulation of non-linear ship motions in irregular seas is possible. Also included in the simulation model are propeller and rudder forces, autopilot and propeller action and control, as well as forces due to wind, longitudinal and transverse resistance, and non-linear roll damping.

Eine Methode zur Simulation von Schiffsbewegungen großer Amplitude im Seegang in sechs Freiheitsgraden wird präsentiert. Starrkörper-Bewegungsgleichungen, die für große Bewegungsampituden geeignet sind, werden hergeleitet. Das Simulationsmodell berücksichtigt alle signifikanten Kräfte, die auf das Schiff wirken. Die Froude-Krilov-Kräfte werden für die tatsächliche Wasserlinie entlang des Schiffskörpers berechnet. Die hydrodynamischen Radiations- und Diffraktionskräfte werden mit Differentialgleichungen höherer Ordnung berechnet, die die Relativbewegung zwischen dem Wasser und den Schiffsquerschnitten in Beziehung zu den Spantkräften setzen. Die hydrodynamischen Koeffizienten werden mit einer linearisierten Methode berechnet, aber in jedem Zeitschritt werden die Werte für die aktuelle getauchte Schiffsform benutzt. Anders als in linearisierten Berechnungen sind die Koeffizienten der Bewegungsgleichungen unabhängig von der Frequenz. Daher ist die Simulation von nichtlinearen Schiffsbewegungen in unregelmäßigem Seegang möglich. Im Simulationsmodell sind auch Propeller- und Ruderkräfte, Regler für Kurs und Propellerdrehzahl sowie Windkräfte, Längs- und Querwiderstand und nichtlineare Rolldämpfung enthalten.

Contents

1 Introduction

The motion of ships in a seaway has always been of great interest to naval architects. The rolling motion is of particular importance since it is directly connected with the problem of safety against capsizing.
One of the first theoretical approaches in this respect is undoubtedly Froude's classical paper "On the Rolling of Ships" [6]. Captain Krilov went a significant step forward in his paper "A General Theory of the Oscillations of a Ship on Waves" [15], where he presents a calculation method for predicting rigid body motions in 6 degrees of freedom. Both Froude and Krilov use the assumption that the waves are not disturbed by the ship's presence, nowadays referred to as the "Froude-Krilov Hypothesis".
With the presentation of the Strip Theory by Korvin-Kroukovsky [14] a major breakthrough in the history of seakeeping prediction methods was achieved. Many enhancements of the Strip Theory have been made by various authors [9, 19, 22] and it can be said that the strip method today is the basic tool for seekeeping predictions. Being a linear method the strip theory obviously has its limitations. While the prediction of heave and pitch is very good, the results for the highly nonlinear phenomenon of the rolling motion are very poor.
Important work in the field of rolling was done by Grim [8], who proved that roll resonance can appear in longitudinal waves. Various authors [1, 13, 17, 18] have used the equation of motion for the uncoupled rolling motion in conjunction with stochastic methods to establish stability criteria for ships rolling in irregular seas.
Normally, though, rolling is coupled to some extent with all other motions, particularly with sway and yaw, and this has to be considered in a prediction method.
Apart from theoretical approaches there were also experimental investigations into the stability of ships in irregular seas. A large series of model experiments was done in the HSVA to investigate the stability of modern container ships [4, 5]. Another comprehensive test program was carried out by SSPA in Göteborg for stern trawlers [10].
With the modern computer technology now available hitherto unthinkable methods can now be employed, since a vast amount of numerical calculations does present less of a problem. One such method is the simulation of ship motions in a seaway. Mathematically a simulation consists of the time domain solution of a set of differential equations describing the behaviour of the ship in response to its environment.
Kröger [16] uses a combination of linear and non-linear methods for simulating ship motions. He uses strip theory results for the heave, pitch, sway, and yaw motion in conjunction with a non-linear equation of motion for rolling. Included in this equation are linear and quadratic damping coefficients, a non-linear, time-dependent righting moment, and external moments due to the waves. Because of the linearized calculation this method cannot simulate broaching in following waves and generally underestimates the yaw-motion.
A different approach for predicting non-linear ship motions in large amplitudes waves is taken by Fujino and Yoon [7]. They use, what can be called a non-linear extension of the strip method, for the simulation of motions in five degrees of freedom, namely heave, pitch, sway, yaw, and roll. The sectional hydrodynamic coefficients are calculated with a linearized method (for small amplitude motions), but at every time-

step the coefficients corresponding to the instantaneous submerged portion of the section are used. Thus the nonlinearity in the hydrodynamic forces stems from the time-variation of the ship's submerged part. The hydrostatic and Froude-Krilov forces are calculated exactly by integrating the water pressure over the instantaneous submerged portion of the vessel's hull. In the linear strip method the response for irregular seas is obtained by using the superposition of responses for regular waves of different frequencies. With non-linear system response this is not possible. Since the hydrodynamic coefficients used by Fujino and Yoon vary with frequency, their method can only be applied to regular waves (where a single motion frequency prevails).

In this paper a method for the simulation of large amplitude (nonlinear) ship motions in all six degrees of freedom is presented. In the simulation model presented here all significant forces acting on a ship in a seaway are included. The Froude-Krilov forces are calculated using the actual waterline along the hull. In a way similar to Fujino's method, the hydrodynamic coefficients for two-dimensional flow within transverse section planes are calculated using a linearised method, but at every time step the values corresponding to the instantaneous submerged shape of the ship are used. For the calculation of radiation and diffraction forces a higher order differential equation is used to take account of the memory effects of the free water surface. Other than in linearised calculations the coefficients of the equations of motion are independent of frequency, which makes the simulation of large amplitude ship motions in irregular waves possible. Non-linear phenomena such as large angle rolling and broaching in following waves can be simulated.

The paper is based on [23], which was a preliminary study for this project. [23] presents a number of concepts and suggests methods for implementing them without going into much detail. In this paper the concepts from [23] are worked out in detail. However, extensive changes of some of the methods proposed in [23] were found to be necessary. The equations of motion had to be changed in order to separate terms depending on acceleration from other terms, thus making a solution possible. The determination of the section waterlines needed for the calculation of both the Froude-Krilov and the radiation and diffraction forces is completely different from the method suggested in [23]. For the calculation of the radiation and diffraction forces a higher order differential equation is used as given in [23]. However, in [23] no method for solving this equation is given. Such a method, together with ways of testing the numerical stability of the higher order differential equation and calculating it's coefficients were developed from scratch. The methods for calculating the rudder, propeller and wind forces are worked out in detail in this paper, while [23] just references the literature.

2 Conventions, Definitions and Basic Equations

2.1 Symbols

Vectors are denoted by lowercase underlined letters (e.g. "$\underline{x}$"). Vectors in the earth coordinate system either have an index ξ (e.g. "$\underline{b}_\xi$") or are denoted by lowercase greek letters. Vectors in the ship coordinate system have no index. Matrices are written as uppercase letters. Scalars are denoted by lowercase letters which are not underlined. The index G indicates that a quantity refers to the centre of gravity of the ship (e.g. "$\underline{x}_G$"). Dots on top of a symbol denote a time derivative.

2.2 Coordinate Systems

Two coordinate systems will be used. One is fixed to the earth and shall henceforth be called "earth coordinate system". Its origin lies in a distance equal to the draught of the ship below the still water surface. Its axes are called ξ, η and ζ. ξ points horizontally in the direction of the mean ship's heading. η points horizontally to starboard. ζ points vertically downward. The second coordinate system is fixed to the ship and shall be called "ship coordinate system". Its origin is located at the keel amidships. The axes are x, y, and z. The x-axis is parallel to the keel and points towards the bow. The y-axis is at right angles to x and parallel to the ship's decks, pointing to starboard. z is at right angles to both x and y, pointing downward.

2.3 Coordinate Transformations

Consider a point

$$\underline{\xi} = \begin{pmatrix} \xi \\ \eta \\ \zeta \end{pmatrix} \tag{2.1}$$

in the earth coordinate system. The same point in the ship coordinate system may be called

$$\underline{x} = \begin{pmatrix} x \\ y \\ z \end{pmatrix} \tag{2.2}$$

$\underline{\xi}$ and $\underline{x}$ are related by the equation

$$\underline{\xi} = T \cdot \underline{x} + \underline{\xi}_o \tag{2.3}$$

$\underline{\xi}_O$ is the position of the origin of the ship coordinate system in the earth coordinate system. T is a transformation matrix representing the rotation of the ship relative to the earth coordinate system. T can be derived from the concatentation of transformations for rotations about each of the three coordinate axes. To make this transformation unequivocal the order of succession of the rotations must be specified. It is as follows:

Rotation about the ξ-axis through the angle φ
Rotation about the η-axis through the angle ϑ
Rotation about the ζ-axis through the angle ψ

Rotation about the ξ-axis, through an angle φ, is achieved by the following transformation:

$$\underline{\xi} = T_1 \cdot \underline{x} = \begin{bmatrix} 1 & 0 & 0 \\ 0 & \cos\varphi & -\sin\varphi \\ 0 & \sin\varphi & \cos\varphi \end{bmatrix} \cdot \underline{x} \qquad (2.4)$$

The rotation angle φ is measured clockwise when looking from the origin in the direction of the positive ξ-axis. For the ship a positive rotation angle φ or angle of heel means a deeper immersion of the starboard side in the water.
Rotation about the η-axis through an angle ϑ is given by:

$$\underline{\xi} = T_2 \cdot \underline{x} = \begin{bmatrix} \cos\vartheta & 0 & \sin\vartheta \\ 0 & 1 & 0 \\ -\sin\vartheta & 0 & \cos\vartheta \end{bmatrix} \cdot \underline{x} \qquad (2.5)$$

A positive angle ϑ (trim) leads to a deeper immersion of the stern of the ship.
Rotation about the ζ-axis through an angle ψ is given by:

$$\underline{\xi} = T_3 \cdot \underline{x} = \begin{bmatrix} \cos\psi & -\sin\psi & 0 \\ \sin\psi & \cos\psi & 0 \\ 0 & 0 & 1 \end{bmatrix} \cdot \underline{x} \qquad (2.6)$$

A positive angle ψ (yaw) for the ship means a course deviation to starboard. Concatenation of these three transformations is achieved by the product of the transformation matrices. Thus the single transformation matrix T for a combination of all three rotations can be derived:

$$T = T_3 \cdot T_2 \cdot T_1 = \begin{bmatrix} \cos\psi\cos\vartheta & -\cos\varphi\sin\psi+\sin\varphi\cos\psi\sin\vartheta & \sin\varphi\sin\psi+\cos\varphi\cos\psi\sin\vartheta \\ \sin\psi\cos\vartheta & \cos\varphi\cos\psi+\sin\varphi\sin\psi\sin\vartheta & -\sin\varphi\cos\psi+\cos\varphi\sin\psi\sin\vartheta \\ -\sin\vartheta & \sin\varphi\cos\vartheta & \cos\varphi\cos\vartheta \end{bmatrix} \qquad (2.7)$$

T can also be written in the following simplified ways:

$$T = \begin{bmatrix} t_{11} & t_{12} & t_{13} \\ t_{21} & t_{22} & t_{23} \\ t_{31} & t_{32} & t_{33} \end{bmatrix} = \begin{bmatrix} \underline{t}_1 \\ \underline{t}_2 \\ \underline{t}_3 \end{bmatrix} = [\underline{t}_4, \underline{t}_5, \underline{t}_6] \qquad (2.8)$$

As can be shown easily the inverse of the transformation matrix is equal to the transposed transformation matrix:

$$T^{-1} = T^T \qquad (2.9)$$

2.4 Velocities

The velocity is the time derivative of the position vector:

$$\dot{\underline{\xi}} = \frac{\partial \underline{\xi}}{\partial t} \tag{2.10}$$

The velocity relative to the earth coordinate system of a point $\underline{x}$ fixed to the ship is

$$\dot{\underline{\xi}} = \dot{T} \cdot \underline{x} + \dot{\underline{\xi}}_O \tag{2.11}$$

The angular velocity is defined as:

$$\underline{\omega} = \begin{pmatrix} \omega_\xi \\ \omega_\eta \\ \omega_\zeta \end{pmatrix} \tag{2.12}$$

The components of this vector are the angular velocities about the axes of the earth coordinate system. From this definition follows:

$$\dot{\underline{\xi}} = \underline{\omega} \times (\underline{\xi} - \underline{\xi}_O) + \dot{\underline{\xi}}_O \tag{2.13}$$

The vector product in this equation can alternatively be written using a matrix multiplication:

$$\dot{\underline{\xi}} = \Omega \cdot (\underline{\xi} - \underline{\xi}_O) + \dot{\underline{\xi}}_O \tag{2.14}$$

where Ω is defined as

$$\Omega = \begin{bmatrix} 0 & -\omega_\zeta & \omega_\eta \\ \omega_\zeta & 0 & -\omega_\xi \\ -\omega_\eta & \omega_\xi & 0 \end{bmatrix} \tag{2.15}$$

According to (2.3) the expression $(\underline{\xi} - \underline{\xi}_O)$ in (2.14) can be replaced by $T \cdot \underline{x}$:

$$\dot{\underline{\xi}} = \Omega \cdot T \cdot \underline{x} + \dot{\underline{\xi}}_O \tag{2.16}$$

Comparing this equation with (2.11) one obtains:

$$\dot{T} = \Omega \cdot T \tag{2.17}$$

Using this equation the numerical integration of T is possible (using a method for the integration of a system of ordinary differential equations, e.g. Runge-Kutta), if starting values for T and the time history of $\underline{\omega}$ are known. Compared with the time integration of the angles φ, ϑ, and ψ this has the advantage that T need not be calculated from these angles at every time step. It may, however, lead to the accumulation of numerical errors in T, making it equivocal. Therefore T is corrected every 30 time steps (the angles are calculated from T, then T is recalculated from (2.7) using these angles).

3 Equations of Motion

For the purpose of simulating ship motions in a seaway the ship can be thought to be a rigid body. The influence of elastic deformations of the ship hull on its motions is considered to be small and will therefore be neglected.

For calculating the accelerations in all 6 degrees of freedom a system of six scalar equations will be set up.
According to Newton's law the time derivative of the momentum $\underline{b}_\xi$ is equal to the force in the earth coordinate system:

$$\dot{\underline{b}}_\xi = \underline{f}_\xi = T \cdot \underline{f} \tag{3.1}$$

T is the transformation matrix, $\underline{f}$ is the force. $\underline{b}_\xi$ and $\underline{f}$ are vectors with 3 elements each. The momentum is defined as the integral over the velocity of every mass element dm of the ship:

$$\underline{b}_\xi = \int_{ship} \dot{\underline{\xi}}\, dm \tag{3.2}$$

With (2.3) this can be written as:

$$\underline{b}_\xi = \dot{T} \cdot \int_{ship} \underline{x}\, dm + \dot{\underline{\xi}}_O \cdot \int_{ship} dm \tag{3.3}$$

From this follows:

$$\underline{b}_\xi = (\dot{T} \cdot \underline{x}_G + \dot{\underline{\xi}}_O) \cdot m \tag{3.4}$$

$\underline{x}_G$ is the vector specifying the position of the centre of gravity, $\dot{\underline{\xi}}_O$ is the translation velocity, m is the ship's mass.
Next follow the equivalent equations for rotation. The moment around the centre of gravity $\underline{d}_{G\xi}$ is equal to the time derivative of the angular momentum $\underline{h}_{G\xi}$ (also with respect to the centre of gravity):

$$\underline{d}_{G\xi} = \dot{\underline{h}}_{G\xi} \tag{3.5}$$

The moment around the coordinate centre is:

$$\underline{d}_\xi = \underline{d}_{G\xi} + (\underline{\xi}_G - \underline{\xi}_O) \times \underline{f}_\xi \tag{3.6}$$

$\underline{d}_\xi$ can be expressed in terms of the moment in the ship coordinate system $\underline{d}$ by $\underline{d}_\xi = T \cdot \underline{d}$. Thus:

$$\underline{d}_{G\xi} = T \cdot \underline{d} - (T \cdot \underline{x}_G) \times \underline{f}_\xi \tag{3.7}$$

From this follows an equation for the time derivative of the angular momentum:

$$\dot{\underline{h}}_{G\xi} = T \cdot \underline{d} - (T \cdot \underline{x}_G) \times \dot{\underline{b}}_\xi \tag{3.8}$$

According to [23] the angular momentum can be expressed by

$$\underline{h}_{G\xi} = T \cdot I_G \cdot T^{-1} \cdot \underline{\omega} \tag{3.9}$$

I_G is the matrix of the moments of inertia relative to the centre of gravity of the ship, defined as:

$$I_G = \begin{bmatrix} I_{Gx} & -I_{Gxy} & -I_{Gxz} \\ -I_{Gxy} & I_{Gy} & -I_{Gyz} \\ -I_{Gxz} & -I_{Gyz} & I_{Gz} \end{bmatrix} \tag{3.10}$$

with

$$I_{Gx} = \int_{ship} [(y - y_G)^2 + (z - z_G)^2]dm \tag{3.11}$$

$$I_{Gxy} = \int_{ship} (x - x_G)\cdot(y - y_G)\,dm \tag{3.12}$$

The other matrix elements are defined accordingly.
The equations for the momentum (3.4) and the angular momentum (3.9) derivated by time are:

$$\dot{\underline{b}}_\xi = (\ddot{T}\cdot\underline{x}_G + \ddot{\underline{\xi}}_O)\cdot m \tag{3.13}$$

$$\dot{\underline{h}}_{G\xi} = (\dot{T}\cdot I_G\cdot T^{-1} + T\cdot I_G\cdot\dot{T}^{-1})\cdot\underline{\omega} + T\cdot I_G\cdot T^{-1}\cdot\dot{\underline{\omega}} \tag{3.14}$$

Combining (3.1) with (3.13) and (3.8) with (3.14) one obtains:

$$(\ddot{T}\cdot\underline{x}_G + \ddot{\underline{\xi}}_O)\cdot m = T\cdot\underline{f} \tag{3.15}$$

$$(\dot{T}\cdot I_G\cdot T^{-1} + T\cdot I_G\cdot\dot{T}^{-1})\cdot\underline{\omega} + T\cdot I_G\cdot T^{-1}\cdot\dot{\underline{\omega}} = T\cdot\underline{d} - (T\cdot\underline{x}_G)\times(\ddot{T}\cdot\underline{x}_G + \ddot{\underline{\xi}}_O)\cdot m \tag{3.16}$$

This is a system of 2 vector equations or 6 scalar equations for calculating the accelerations in the six degrees of freedom. Since the force $\underline{f}$ and the moment $\underline{d}$ depend on the accelerations of the ship, this system of equations cannot be solved as it stands. Force and moment are split up into terms depending on accelerations and others which do not depend on accelerations.

$$\underline{f} = -F_1\cdot\ddot{\underline{u}}_\xi + \underline{f}_2 \tag{3.17}$$

$$\underline{d} = -D_1\cdot\ddot{\underline{u}}_\xi + \underline{d}_2 \tag{3.18}$$

In these equations F_1 and D_1 are 3x6-matrices, which are still to be determined. $\ddot{\underline{u}}_\xi$ is a combination of the translational and rotational acceleration vectors:

$$\ddot{\underline{u}}_\xi = \begin{pmatrix} \dot{\underline{\xi}}_O \\ \dot{\underline{\omega}} \end{pmatrix} \tag{3.19}$$

$\underline{f}_2$ and $\underline{d}_2$ are those parts of the force and moment, which do not depend on any accelerations.

The expressions for $\underline{f}$ and $\underline{d}$ (Equ. 3.17 and 3.18) can be substituted into (3.15) and (3.16):

$$(\ddot{T}\cdot\underline{x}_G + \ddot{\underline{\xi}}_0)\cdot m = T\cdot(-F_1\cdot\ddot{\underline{u}}_\xi + \underline{f}_2) \tag{3.20}$$

$$(\dot{T}\cdot I_G\cdot T^{-1} + T\cdot I_G\cdot \dot{T}^{-1})\cdot\underline{\omega} + T\cdot I_G\cdot T^{-1}\,\dot{\underline{\omega}} =$$

$$T\cdot(-D_1\,\ddot{\underline{u}}_\xi + \underline{d}_2) - (T\cdot\underline{x}_G)\times(\ddot{T}\cdot\underline{x}_G + \ddot{\underline{\xi}}_0)\cdot m \tag{3.21}$$

This set of equations of motion is used in the simulation. It includes all coupling and gyroscopic terms. The forces $\underline{f}_2$ and moments $\underline{d}_2$ can be arbitrary functions of time, velocity, and position of the vessel. Only the forces and moments depending on the accelerations are presupposed to be linear functions of the accelerations.

The second time derivative of the transformation matrix, $\ddot{T}$, follows from $\dot{T} = \Omega\cdot T$:

$$\ddot{T} = \dot{\Omega}\cdot T + \Omega\cdot\dot{T} = \dot{\Omega}\cdot T + \Omega^2\cdot T \tag{3.22}$$

4 Forces Due to the Ship's Weight

The force due to the ship's weight in the ship coordinate system is:

$$\underline{f}_g = m \cdot g \cdot \underline{t}_3^T \tag{4.1}$$

m is the ship's mass, g is the gravitational acceleration, $\underline{t}_3$ is the lower row vector of the transformation matrix T (ref. equ. 2.8).
The moment due to the ship's weight is:

$$\underline{d}_g = \underline{x}_G \times \underline{f}_g \tag{4.2}$$

where $\underline{x}_G$ is the position of the ship's centre of gravity in the ship coordinate system.

5 Froude-Krilov-Forces

5.1 Introduction

Froude-Krilov-Forces are those forces which would act upon a ship, if the waves were not disturbed by the ship's presence.

5.2 Representation of the Seaway

The seaway is represented by a sum of sine waves according to the following formula:

$$\zeta_S(\xi,\eta,t) = -d + \sum_j \zeta_j \cdot \cos(\omega_j \cdot t - k_j \cdot \xi \cdot \cos\mu_j + k_j \cdot \eta \cdot \sin\mu_j + \varepsilon_j) \tag{5.1}$$

ζ_S is the height of the water surface at the position (ξ,η) and the time t. d is the ship's mean draught. ζ_j is the amplitude of component wave j, ω_j is the circular frequency, μ_j is the wave direction (0° for waves from aft, 90° for waves from starboard), ε_j is the phase angle. k_j is the wave number ω_j^2/g.

5.3 Corrected Waterline

The Froude-Krilov-Forces will not be calculated using the actual pressure distribution on the ship's hull. Instead the hydrostatic pressure distribtion up to a corrected waterline is used. To further simplify the calculation, this corrected waterline is approximated by a straight line in the section planes.

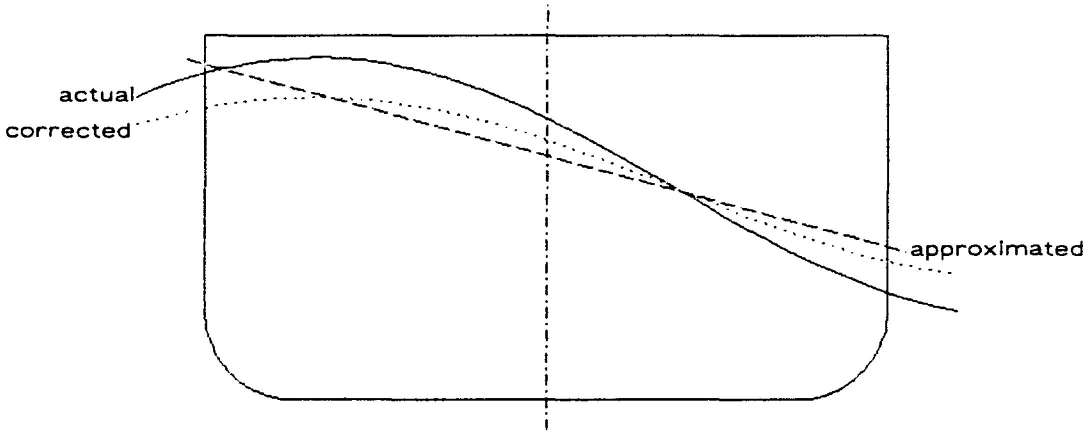

Figure 5-1: Actual, corrected and approximated waterlines at a section

Instead of integrating the pressure over the hull surface, one can now use simple hydrostatic calculations for the determination of the section force and moment.
The corrected height of the water surface is determined from an equation like (5.1) with wave amplitudes ζ_j replaced by reduced amplitudes ζ_{j1}:

$$\zeta_{j1} = \zeta_j \cdot e^{-k_j \cdot z_1} \tag{5.2}$$

Since the pressure variation on the bottom of the section is of interest here, z_1 is taken as the instantaneous draught of the respective section (this is, of course, not known beforehand, but can be approximated very well by the value from the previous time step).

The corrected waterline is to be approximated by a straight line in the section plane. The height of this straight line at the centre of the section waterline can be calculated by introducing an approximation factor r_{j1} into the equation for the wave height:

$$\zeta_{S1}(\xi,\eta,t) = -d + \sum_j \zeta_{j1}\cdot r_{j1}\cdot\cos(\omega_j\cdot t - k_j\cdot\xi\cdot\cos\mu_j + k_j\cdot\eta\cdot\sin\mu_j + \varepsilon_j) \qquad (5.3)$$

Similarly the inclinations of the water surface in ξ- and η-direction at the centre of the section waterline which are to be used for determining the slope of the straight line are calculated using a factor r_{j2}:

$$\frac{\partial\zeta}{\partial\xi} = \sum_j \zeta_{j1}\cdot r_{j2}\cdot k_j\cdot\cos\mu_j\cdot\sin(\omega_j\cdot t - k_j\cdot\xi\cdot\cos\mu_j + k_j\cdot\eta\cdot\sin\mu_j + \varepsilon_j) \qquad (5.4)$$

$$\frac{\partial\zeta}{\partial\eta} = -\sum_j \zeta_{j1}\cdot r_{j2}\cdot k_j\cdot\sin\mu_j\cdot\sin(\omega_j\cdot t - k_j\cdot\xi\cdot\cos\mu_j + k_j\cdot\eta\cdot\sin\mu_j + \varepsilon_j) \qquad (5.5)$$

The calculation of the factors r_{j1} and r_{j2} is described in appendix B. With these factors the slope in the section planes (x = const.) is given with good accuracy while the slope in the x-direction is given with less accuracy.

5.4 Immersion of a section

For the approximation of the waterline in the section planes correction factors r_{j1} and r_{j2} were introduced. These depend on the half breadth of the waterline b and are only valid if wave height and inclination are determined at the midpoint of the section waterline $\underline{x}_m$. b and $\underline{x}_m$ are of course unknown at the start of the calculation. Therefore an iterative process is necessary which starts with the values from the previous time step. At the first time step the values for the equilibrium position of the ship in still water are used.

The point $\underline{x}_m$ is transformed to the earth coordinate system, yielding $\underline{\xi}_1 = (\xi_1,\eta_1,\zeta_1)$. At the position given by ξ_1 and η_1 the height of the water surface ζ_s and the inclinations of the waterline in ξ- and η-direction, $\partial\zeta/\partial\xi$ and $\partial\zeta/\partial\eta$, are calculated using values for the correction factors r_{j1} and r_{j2} based on b and $\underline{x}_m$ from the previous time step.

An equation of the plane through the point $\underline{\xi}_2 = (\xi_1,\eta_1,\zeta_s)$ with the inclinations $\partial\zeta/\partial\xi$ and $\partial\zeta/\partial\eta$ (later also referred to as the waterplane) is:

$$\underline{\xi}_{p1} = \underline{\xi}_2 + \tau_1\cdot\begin{pmatrix}1\\0\\\partial\zeta/\partial\xi\end{pmatrix} + \tau_2\cdot\begin{pmatrix}0\\1\\\partial\zeta/\partial\eta\end{pmatrix} \qquad (5.6)$$

Here τ_1 and τ_2 are parameters specifying different points on the plane.

The line of intersection between this plane and the section plane can then be calculated. This line is considered the new section waterline. There is, of course, an error involved in calculating the waterline in this way. This error depends on the distance of the point $\underline{\xi}_2$ from the section plane. The larger this distance, the larger is the error. The distance is a function of the pitch angle. When the pitch angle is zero the distance and the error are also zero.
An equation for the section plane in the ship coordinate system is:

$$\underline{x}_{ps} = \begin{pmatrix} x_s \\ 0 \\ 0 \end{pmatrix} + \lambda_1 \cdot \begin{pmatrix} 0 \\ 1 \\ 0 \end{pmatrix} + \lambda_2 \cdot \begin{pmatrix} 0 \\ 0 \\ 1 \end{pmatrix} \tag{5.7}$$

Since the equation of the line of intersection is required in the ship coordinate system, it is appropriate to convert the equation of the waterplane to this coordinate system.

$$\underline{x}_{p1} = T^{-1} \cdot (\underline{\xi}_{p1} - \underline{\xi}_0) \tag{5.8}$$

$$\underline{x}_{p1} = T^{-1} \cdot (\underline{\xi}_2 - \underline{\xi}_0) + \tau_1 \cdot T^{-1} \cdot \begin{pmatrix} 1 \\ 0 \\ \partial\zeta/\partial\xi \end{pmatrix} + \tau_2 \cdot T^{-1} \cdot \begin{pmatrix} 0 \\ 1 \\ \partial\zeta/\partial\eta \end{pmatrix} \tag{5.9}$$

This can be simplified by introducing new vectors $\underline{x}_2$, $\underline{v}_1$, and $\underline{v}_2$.

$$\underline{x}_{p1} = \underline{x}_2 + \tau_1 \cdot \underline{v}_1 + \tau_2 \cdot \underline{v}_2 \tag{5.10}$$

The condition for the intersection is $x_{p1} = x_{ps}$, from which follows:

$$x_s = x_2 + \tau_1 \cdot v_{1x} + \tau_2 \cdot v_{2x} \tag{5.11}$$

Here v_{1x} and v_{2x} are the x-components of $\underline{v}_1$ and $\underline{v}_2$ respectively. From this equation follows:

$$\tau_2 = \frac{x_s - x_2 - \tau_1 \cdot v_{1x}}{v_{2x}} = \frac{x_s - x_2}{v_{2x}} - \tau_1 \cdot \frac{v_{1x}}{v_{2x}} \tag{5.12}$$

or alternatively

$$\tau_1 = \frac{x_s - x_2 - \tau_1 \cdot v_{2x}}{v_{1x}} = \frac{x_s - x_2}{v_{1x}} - \tau_1 \cdot \frac{v_{2x}}{v_{1x}} \tag{5.13}$$

Obviously the first of these equations cannot be used, if v_{2x} is zero, and the second one cannot be used, if v_{1x} is zero. So if either v_{1x} or v_{2x} is zero, the appropriate equation must be used. If both v_{1x} and v_{2x} are zero, there is no solution, that is to say there is no intersection, which means that both planes are parallel.
The equation of the intersecting line (for $v_{2x} \neq 0$) is:

$$\underline{x}_i = \underline{x}_2 + \tau_1 \cdot \underline{v}_1 + \left(\frac{x_s - x_2}{v_{2x}} - \tau_1 \cdot \frac{v_{1x}}{v_{2x}}\right) \cdot \underline{v}_2 \tag{5.14}$$

or

$$\underline{x}_i = \underline{x}_2 + \frac{x_s - x_2}{v_{2x}} \cdot \underline{v}_2 + \tau_1 \cdot \left(\underline{v}_1 - \frac{v_{1x}}{v_{2x}} \cdot \underline{v}_2\right) \tag{5.15}$$

which can be written in a simplified way as:

$$\underline{x}_i = \underline{x}_3 + \tau_1 \cdot \underline{v}_3 \tag{5.16}$$

The equivalent equations for $v_{1x} \neq 0$ are:

$$\underline{x}_i = \underline{x}_2 + \left(\frac{x_s - x_2}{v_{1x}} - \tau_2 \cdot \frac{v_{2x}}{v_{1x}}\right) + \tau_2 \cdot \underline{v}_2 \tag{5.17}$$

$$\underline{x}_i = \underline{x}_2 + \frac{x_s - x_2}{v_{1x}} \cdot \underline{v}_1 + \tau_2 \cdot \left(\underline{v}_2 - \frac{v_{2x}}{v_{1x}} \cdot \underline{v}_1\right) \tag{5.18}$$

$$\underline{x}_i = \underline{x}_3 + \tau_2 \cdot \underline{v}_3 \tag{5.19}$$

In the section coordinate system y-z this line can be expressed by

$$\begin{pmatrix} y_i \\ z_i \end{pmatrix} = \begin{pmatrix} y_3 \\ z_3 \end{pmatrix} + \tau_1 \cdot \begin{pmatrix} v_{3y} \\ v_{3z} \end{pmatrix} \tag{5.20}$$

This parameter equation can be converted to

$$z = \frac{v_{3z}}{v_{3y}} \cdot y + \left(z_3 - \frac{v_{3z}}{v_{3y}} \cdot y_3\right) \tag{5.21}$$

The points of intersection of this line and the section contour can now be calculated. From these one can obtain new values for the waterline breadth and the position of the midpoint, calculate new values of r_{j1} and r_{j2}, and restart the iteration. This iterative process must be carried on until the improvement in each step falls below a given limit.

The computation time needed to calculate the points of intersection of waterline and section contour can be reduced, if a simplified section contour is used. For ordinary ship sections sufficient accuracy may be achieved by using a simple box shape for approximating the section contour. It must be emphasized that such an approximation does not affect the calculation of the immersed area and righting moment. It is only used for finding appropriate correction factors r_{j1} and r_{j2} and the height and slope of the waterline. The section area and righting moment are then calculated for the *real* section.

For reasons of computational efficiency the actual calculation of the immersed area and righting moment is not done during the simulation. Instead these values are calculated in advance for a number of draughts and inclinations of the waterline for every ship section and stored in computer memory. During the simulation the actual values are interpolated from this table.

The procedure outlined in this section leaves room for improvement. There are inaccuracies in the determination of the slope of the water surface in the ship's longitudinal direction and in the calculation of the section waterline for large pitch angles. The latter point could be remedied by extending the iteration process in such a way, that the point $\underline{\xi}_2$ came to lie in the section plane. However, since this whole method appears rather lengthy and complicated, it might not be a bad idea to discard it altogether and to calculate the Froude-Krilov forces exactly, even if this meant an increase in the required computation time.

5.5 Ship's Wave Profile

The wave profile due to the ship's forward speed is calculated using a formula given in [4] for a ship moving in still water:

$$\frac{\xi}{L} = 0.442 \cdot F_n^4 \cdot \cos\left(\frac{1 - 2 \cdot F^2 - 2x/l}{2 \cdot F_n^2}\right) - (0.082 + 0.025 \cdot x/l) \cdot F_n^2 \cdot \cos\left(4\pi (x/l)^2\right) \tag{5.22}$$

The height of this wave profile is added to the wave height of the seaway to obtain the total wave height at the ship's sections. Although this formula is only valid for a ship moving in still water and doesn't appear to give correct results for Froude numbers above 0.35 it is used here, because of its simplicity. More accurate methods would be out of place here, because they would waste too much computation time.

5.6 Force and Moment

For the calculation of the force and moment vectors the angle λ between the perpendicular on the waterplane and the x-axis is required. The unit vector perpendicular to the waterplane is given by:

$$\underline{n}_p = -\frac{1}{\sqrt{1 + \left(\frac{\partial\zeta}{\partial\xi}\right)^2 + \left(\frac{\partial\zeta}{\partial\eta}\right)^2}} \cdot \begin{pmatrix} \partial\zeta/\partial\xi \\ \partial\zeta/\partial\eta \\ 1 \end{pmatrix} \tag{5.23}$$

The vector in the direction of the x-axis is equal to the first column vector $\underline{t}_4$ of the transformation matrix. The cosine of the angle between $\underline{n}_p$ and $\underline{t}_4$ is given by the scalar product

$$\cos\lambda = \underline{t}_4 \cdot \underline{n}_p = \frac{-\left(t_{11} \cdot \frac{\partial\zeta}{\partial\xi} + t_{21} \cdot \frac{\partial\zeta}{\partial\eta} + t_{31}\right)}{\sqrt{1 + \left(\frac{\partial\zeta}{\partial\xi}\right)^2 + \left(\frac{\partial\zeta}{\partial\eta}\right)^2}} \tag{5.24}$$

The force and moment vectors can then be integrated over the ship's length l (acc. to [23]).

$$\underline{f}_F = \rho g \int_l \begin{pmatrix} a_s \cdot \cos\lambda \\ -a_s \cdot \sin\varphi_1 \cdot \sin\lambda \\ -a_s \cdot \cos\varphi_1 \cdot \sin\lambda \end{pmatrix} dx \tag{5.25}$$

$$\underline{d}_F = \rho g \int_l \begin{pmatrix} m_s \cdot \sin\lambda \\ a_s \cdot \cos\varphi_1 \cdot \sin\lambda \cdot x \\ -a_s \cdot \sin\varphi_1 \cdot \sin\lambda \cdot x \end{pmatrix} dx \tag{5.26}$$

The immersed area a_s and the area moment m_s around the x-axis of the sections are interpolated from a table of previously calculated values for the instantaneous depth of immersion and angle of the waterline φ_1.

6 Radiation and Diffraction Forces

6.1 Introduction

Radiation forces result from the motion of the ship in calm water (radiation of waves). Diffraction forces are caused by the disturbance of the waves due to the ship, with the ship imagined not to move in the earth system except for a constant forward speed. Both forces can in good approximation be calculated jointly as functions of the relative motion between the ship and the undisturbed waves.

6.2 Frequency Domain Representation

Let us first look at the two-dimensional flow around a partly submerged ship's section. In this case the pressure distribution can be determined by potential theory, the flow being represented by a distribution of time periodic sources and sinks.
The relative motion between ship and water in the transverse and vertical directions and the relative section rotation are combined in a vector $\underline{u}_x$:

$$\underline{u}_x = \begin{pmatrix} \text{relative motion of the section keel point (x,0,0) in y-direction} \\ \text{relative motion of the keel point in z-direction} \\ \text{relative rotation around the x-axis} \end{pmatrix} \tag{6.1}$$

A vector $\underline{f}_x$ is used to represent the section force and moment, which result from the pressure along the section contour.

$$\underline{f}_x = \begin{pmatrix} \text{section force in y-direction} \\ \text{section force in z-direction} \\ \text{section moment around the x-axis} \end{pmatrix} \tag{6.2}$$

In the frequency domain $\underline{u}_x$ can be represented as a sum of different regular oscillations with the complex amplitudes $\hat{\underline{u}}_m$ and the circular frequencies ω_m (from [23]):

$$\underline{u}_x = \sum_{m=1}^{mm} \mathrm{Re}(\hat{\underline{u}}_m \cdot e^{i\omega_m t}) \tag{6.3}$$

The force can be represented in a similar way:

$$\underline{f}_x = \sum_{m=1}^{mm} \mathrm{Re}(\hat{\underline{f}}_m \cdot e^{i\omega_m t}) \tag{6.4}$$

According to [23] the complex amplitudes $\hat{\underline{f}}_m$ can be expressed by the added mass matrix M and the damping matrix N:

$$\hat{\underline{f}}_m = [\omega_m^2 \cdot M(\omega_m) - i\omega_m \cdot N(\omega_m)] \cdot \hat{\underline{u}}_m \tag{6.5}$$

6.3 Time Domain Representation

We want to determine the added mass and damping as functions of the actual time-dependant immersion of a section and of the motion frequency. M and N will be calculated for small amplitude motions, but in every instant the values for the actual immersion of the section will be used. Therefore M and N are nonlinear functions of the immersion and of the motion frequency.
The frequency-domain equations cannot be used for a time-domain simulation of nonlinear motions since the superposition principle cannot be applied. Instead a higher order differential equation is used for describing the relationsship between motion and force (an approach also used by Schmiechen [20] and Jefferys [12]):

$$\sum_{j=0}^{jj} A_j \cdot \underline{u}_x^{(j)} = \sum_{k=0}^{kk} B_k \cdot \underline{f}_x^{(k)} \tag{6.6}$$

Here (j) and (k) denote the jth and kth time derivative respectively. A_j and B_j are real 3×3-matrices depending on the immersed shape of the section, but not on frequency. They have to be chosen in such a way, that (6.6) represents the same relationsship as (6.3) to (6.6). Substituting (6.3) and (6.4) into (6.6) one obtains:

$$\sum_{j=0}^{jj} A_j \cdot \sum_{m=1}^{mm} \mathrm{Re}\left[\hat{\underline{u}}_m \cdot (i\omega_m)^j \cdot e^{i\omega_m t}\right] = \sum_{k=0}^{kk} B_k \cdot \sum_{m=1}^{mm} \mathrm{Re}\left[\hat{\underline{f}}_m \cdot (i\omega_m)^k \cdot e^{i\omega_m t}\right] \tag{6.7}$$

Replacing $\hat{\underline{f}}_m$ by (6.5) and rearranging the equation results in:

$$\sum_{m=1}^{mm} \mathrm{Re}\left\{ e^{i\omega_m t} \left(\sum_{j=0}^{jj} A_j \cdot (i\omega_m)^k\right) \cdot \hat{\underline{u}}_m \right\} =$$

$$\sum_{m=1}^{mm} \mathrm{Re}\left\{ e^{i\omega_m t} \left[\sum_{k=0}^{kk} B_k \cdot (i\omega_m)^k\right] \cdot \left[\omega_m^2 \cdot M(\omega_m) - i\omega_m \cdot N(\omega_m)\right] \cdot \hat{\underline{u}}_m \right\} \tag{6.8}$$

This equation is valid for all times t, if the following equation holds for all frequencies ω_m:

$$\sum_{j=0}^{jj} A_j \cdot (i\omega_m)^j = \left[\sum_{k=0}^{kk} B_k \cdot (i\omega_m)^k\right] \cdot \left[\omega_m^2 \cdot M(\omega_m) - i\omega_m \cdot N(\omega_m)\right] \tag{6.9}$$

Since this is a homogeneous equation, one of the matrices A and B can be chosen freely. Therefore B_{kk} is set equal to the unit matrix E.
For ω_m going towards infinity the factor $[\omega_m \cdot M(\omega_m) - i\omega_m \cdot N(\omega_m)]$ will become $-\omega_m \cdot M\infty$ ($M\infty$ is the added mass for infinite frequency). In this case the left and right hand sides of the equation can only be equal, if jj = kk+2.
For $\omega_m = 0$ the right hand side of the equation equals zero. The left hand side can only be zero, if $A_0 = 0$ (3×3-zero-matrix).
If both sides of the equation are divided by $i\omega_m$ and $\omega_m = 0$, then A_1 must be equal to the zero-matrix.
After renaming the indices (6.6) and (6.9) can be written as:

$$\sum_{k=0}^{kk} A_k \cdot \underline{u}_x^{(k+2)} = \sum_{k=0}^{kk} B_k \cdot \underline{f}_x^{(k)} \tag{6.10}$$

$$\left[\sum_{k=0}^{kk} B_k \cdot (i\omega)^k\right]^{-1} \cdot \sum_{k=0}^{kk} A_k \cdot (i\omega)^{k+2} \approx \left[\omega^2 \cdot M(\omega) - i\omega \cdot N(\omega)\right], \text{ for } 0 \le \omega \le \infty \tag{6.11}$$

Here the equals-sign (=) is replaced by an approximately-equals-sign (≈) since equality of both sides of this equation cannot be achieved using a finite number of coefficients A and B. A method for determining the A and B from (6.11) is given in appendix C.

6.4 Three-Dimensional Flow

The flow around a moving ship is, of course, three-dimensional. Therefore (6.10) has to be modified to include the effect of the ship's forward motion. This is done in analogy to the strip method. The time derivatives are replaced by the differential operator D, defined as:

$$D = \frac{\partial}{\partial t} - v_x \cdot \frac{\partial}{\partial x}$$

This is an approximation which has been used with good results in strip theory.
(6.10) thus becomes:

$$\sum_{k=0}^{kk} D^{k+1}(A_k \cdot \underline{\dot{u}}_x) = \sum_{k=0}^{kk} D^k (B_k \cdot \underline{f}_x) \tag{6.12}$$

The matrices A_k and B_k are included in the differentiation in analogy with the strip method, where the added mass and damping are also differentiated. A modification of this equation is necessary in the event of flow separation. This is treated in section 6.6.

Matrices A_k and B_k will be calculated for a number of sections and for different depths of immersion and angles of inclination. During the simulation they are determined for the instantaneous draught and slope of the waterline.
Matrices A and B cannot, however, be interpolated from the table of values calculated in advance, because in (6.11) a matrix inversion is performed. Therefore interpolation can lead to large errors, unless the interpolation method is specifically adapted to this problem. Even if an interpolation leading to minor errors is used, the resulting matrices A and B may have such properties, that the simulation would become unstable. Since the stability test (described in section 6.7) requires too much computation time, it cannot be performed during the simulation. To avoid these difficulties matrices A and B are taken from the previously calculated table for values of draught and inclination angle next to the actual values. This method has the additional advantage that the computation time needed for establishing the A- and B-values is much lower than for any interpolation process.

6.5 Solving the Higher Order Differential Equation

Equation (6.12) is integrated substantially kk times:

$$\sum_{k=0}^{kk} D^{k+1-L}(A_k \cdot \underline{\dot{u}}_x) = \sum_{k=0}^{kk} D^{k-L} (B_k \cdot \underline{f}_x) \tag{6.13}$$

Here a negative subscript denotes a substantial integration, which is the opposite of a substantial derivative $D = (\partial/\partial t - v \cdot \partial/\partial x)$. The equation can also be written in the following way:

$$\sum_{k=0}^{kk-2} D^{k+1-L}(A_k \cdot \underline{\dot{u}}_x) + A_{L-1} \cdot \underline{\dot{u}}_x + D(A_L \cdot \underline{\dot{u}}_x) = \sum_{k=0}^{kk-1} D^{k-L}(B_k \cdot \underline{f}_x) + B_L \cdot \underline{f}_x \qquad (6.14)$$

With $B_{kk} = E$ the following expression for $\underline{f}_x$ can be derived:

$$\underline{f}_x = \sum_{k=0}^{kk-2} D^{k+1-kk} A_k \cdot \underline{\dot{u}}_x) - \sum_{k=0}^{kk-1} D^{k-kk} B_k \cdot \underline{f}_x) + A_{kk-1} \cdot \underline{\dot{u}}_x + D(A_{kk} \cdot \underline{\dot{u}}_x) \qquad (6.15)$$

For kk = 3 this is equal to:

$$\underline{f}_x = -D^{-3}(B_0 \cdot \underline{f}_x) + D^{-2}(A_0 \cdot \underline{\dot{u}}_x - B_1 \cdot \underline{f}_x) + D^{-1}(A_1 \cdot \underline{\dot{u}}_x - B_2 \cdot \underline{f}_x) +$$

$$+ A_2 \cdot \underline{\dot{u}}_x + D(A_3 \cdot \underline{\dot{u}}_x) \qquad (6.16)$$

The right hand side terms in the first line of this equation are combined to a state vector $\underline{s}_1$:

$$\underline{f}_x = \underline{s}_1 + A_2 \cdot \underline{\dot{u}}_x + D(A_3 \cdot \underline{\dot{u}}_x) \qquad (6.17)$$

The derivative of $\underline{s}_1$ is:

$$D\,\underline{s}_1 = -D^{-2}(B_0 \cdot \underline{f}_x) + D^{-1}(A_0 \cdot \underline{\dot{u}}_x - B_1 \cdot \underline{f}_x) + (A_1 \cdot \underline{\dot{u}}_x - B_2 \cdot \underline{f}_x) \qquad (6.18)$$

A second state vector $\underline{s}_2$ is introduced, yielding:

$$D\,\underline{s}_1 = \underline{s}_2 + A_1 \cdot \underline{\dot{u}}_x - B_2 \cdot \underline{f}_x \qquad (6.19)$$

In turn, the derivative of $\underline{s}_2$ is:

$$D\,\underline{s}_2 = -D^{-1}(B_0 \cdot \underline{f}_x) + (A_0 \cdot \underline{\dot{u}}_x - B_1 \cdot \underline{f}_x) \qquad (6.20)$$

Using a third state vector $\underline{s}_3$ this can be written as:

$$D\,\underline{s}_2 = \underline{s}_3 + A_0 \cdot \underline{\dot{u}}_x - B_1 \cdot \underline{f}_x \qquad (6.21)$$

The derivative of $\underline{s}_3$ is:

$$D\,\underline{s}_3 = -B_0 \cdot \underline{f}_x \qquad (6.22)$$

Thus the higher order differential equation is transformed into several first order differential equations in the differential operator D. For the purpose of using an ordinary time integration method to solve these equations the time derivatives of the state vectors are required. They are:

$$\frac{\partial}{\partial t}\underline{s}_1 = \underline{s}_2 + A_1 \cdot \underline{\dot{u}}_x - B_2 \cdot \underline{f}_x + v\frac{\partial}{\partial x}\underline{s}_1 \qquad (6.23)$$

$$\frac{\partial}{\partial t}\underline{s}_2 = \underline{s}_3 + A_0 \cdot \underline{\dot{u}}_x - B_1 \cdot \underline{f}_x + v\frac{\partial}{\partial x}\underline{s}_2 \qquad (6.24)$$

$$\frac{\partial}{\partial t}\underline{s}_3 = -B_0 \cdot \underline{f}_x + v\frac{\partial}{\partial x}\underline{s}_3 \qquad (6.25)$$

The time integration of these equations is executed by a fourth order Runge-Kutta method. The derivatives in x-direction are calculated numerically.

For arbitrary kk equation 6.17 becomes

$$\underline{f}_x = \underline{s}_1 + A_{kk-1}\cdot\underline{\dot{u}}_x + D(A_{kk}\cdot\underline{\dot{u}}_x) \tag{6.26}$$

The last term in this equation can also be written as

$$\begin{aligned}(\frac{\partial}{\partial t} - v\frac{\partial}{\partial x})(A_{kk}\cdot\underline{\dot{u}}_x) &= \frac{\partial}{\partial t}(A_{kk}\cdot\underline{\dot{u}}_x) - v\frac{\partial}{\partial x}(A_{kk}\cdot\underline{\dot{u}}_x) \\ &= \dot{A}_{kk}\cdot\underline{\dot{u}}_x + A_{kk}\cdot\underline{\ddot{u}}_x - v\frac{\partial}{\partial x}(A_{kk}\cdot\underline{\dot{u}}_x)\end{aligned} \tag{6.27}$$

This leads to the following expression for $\underline{f}_x$:

$$\underline{f}_x = \underline{s}_1 + A_{kk-1}\cdot\underline{\dot{u}}_x + \dot{A}_{kk}\cdot\underline{\dot{u}}_x + A_{kk}\cdot\underline{\ddot{u}}_x - v\cdot\frac{\partial}{\partial x}(A_{kk}\cdot\underline{\dot{u}}_x) \tag{6.28}$$

In this equation $\underline{f}_x$ is a function of $\underline{\dot{u}}_x$, that is the relative velocity in the ship coordinate system. For the calculation of the accelerations in the earth coordinate system a transformation is necessary. This is achieved by the following equation:

$$\underline{\dot{u}}_x = W(x)\cdot\underline{\dot{u}}_\xi - \underline{\dot{u}}_{Orb} \tag{6.29}$$

$\underline{\dot{u}}_{Orb}$ is the orbital velocity of the waves in the earth coordinate system (the calculation of the orbital velocity is described in appendix D). W(x) is the following transformation matrix (taken from [23]):

$$W(x) = \begin{bmatrix} t_{12} & t_{22} & t_{32} & (t_{32}t_{21}-t_{22}t_{31})x & (t_{12}t_{31}-t_{32}t_{11})x & (t_{22}t_{11}-t_{12}t_{21})x \\ t_{13} & t_{23} & t_{33} & (t_{33}t_{21}-t_{23}t_{31})x & (t_{13}t_{31}-t_{33}t_{11})x & (t_{23}t_{11}-t_{13}t_{21})x \\ 0 & 0 & 0 & t_{11} & t_{21} & t_{31} \end{bmatrix} \tag{6.30}$$

From (6.29) follows:

$$\underline{\ddot{u}}_x = \dot{W}(x)\cdot\underline{\dot{u}}_\xi + W(x)\cdot\underline{\ddot{u}}_\xi - \underline{\ddot{u}}_{Orb} \tag{6.31}$$

With (6.31) $\underline{f}_x$ can be written as a function of the acceleration $\underline{\ddot{u}}_\xi$ in the earth coordinate system:

$$\begin{aligned}\underline{f}_x = \underline{s}_1 + A_{kk-1}\cdot\underline{\dot{u}}_x + \dot{A}_{kk}\cdot\underline{\dot{u}}_x + A_{kk}\cdot(\dot{W}(x)\cdot\underline{\dot{u}}_\xi + W(x)\cdot\underline{\ddot{u}}_\xi - \underline{\ddot{u}}_{Orb}) + \\ - v\cdot\frac{\partial}{\partial x}(A_{kk}\cdot\underline{\dot{u}}_x)\end{aligned} \tag{6.32}$$

$\underline{f}_x$ is split up into one part $\underline{f}_{xa}$, depending on the acceleration $\underline{\ddot{u}}_\xi$, and the rest $\underline{f}_{xr}$.

$$\underline{f}_x = \underline{f}_{xa} + \underline{f}_{xr} \tag{6.33}$$

$$\underline{f}_{xa} = A_{kk}\cdot W(x)\cdot\underline{\ddot{u}}_\xi \tag{6.34}$$

$$\begin{aligned}\underline{f}_{xr} = \underline{s}_1 + A_{kk-1}\cdot\underline{\dot{u}}_x + \dot{A}_{kk}\cdot\underline{\dot{u}}_x + A_{kk}\cdot(W(x)\cdot\underline{\dot{u}}_\xi - \underline{\ddot{u}}_{Orb}) + \\ - v\cdot\frac{\partial}{\partial x}(A_{kk}\cdot\underline{\dot{u}}_x)\end{aligned} \tag{6.35}$$

Section forces $\underline{f}_x$ are integrated over the ship's length l to obtain the total radiation and diffraction forces:

$$\begin{bmatrix} \underline{f}_B \\ \underline{d}_B \end{bmatrix} = \int_l (V(x) \cdot \underline{f}_x)\, dx \tag{6.36}$$

V(x) is a transformation matrix defined as follows:

$$V(x) = \begin{bmatrix} 0 & 0 & 0 \\ 1 & 0 & 0 \\ 0 & 1 & 0 \\ 0 & 0 & 1 \\ 0 & -x & 0 \\ x & 0 & 0 \end{bmatrix} \tag{6.37}$$

Using equation (6.33) the radiation and diffraction forces can be written as:

$$\begin{bmatrix} \underline{f}_B \\ \underline{d}_B \end{bmatrix} = \int_l (V(x) \cdot \underline{f}_{xa})dx \; + \int_l (V(x) \cdot \underline{f}_{xr})dx \tag{6.38}$$

In this equation the forces are split up as in equations (3.17) and (3.18). Defining V_f as a matrix containing the first three rows of V, and V_d containing the last three rows of V, expressions for F_1, D_1, $\underline{f}_2$, and $\underline{d}_2$ can be derived.

$$F_1 = \int_l (V_f \cdot A_{kk} \cdot W(x))dx \tag{6.39}$$

$$D_1 = \int_l (V_d(x) \cdot A_{kk} \cdot W(x))dx \tag{6.40}$$

$$\underline{f}_2 = \int_l (V_f \cdot \underline{f}_{xr})dx \; + \underline{f}_{other} \tag{6.41}$$

$$\underline{d}_2 = \int_l (V_d(x) \cdot \underline{f}_{xr})dx + \underline{d}_{other} \tag{6.42}$$

$\underline{f}_{other}$ and $\underline{d}_{other}$ are the sum of all other forces and moments.

6.6 Special Treatment of the Case of Flow Separation

When flow separation occurs (6.12) must be modified. Let us first consider the sway and yaw motion. We assume that flow separation occurs at the trailing edge of the hull at the position x_T (for usual ships this is the point where the keel rises, in front of the propeller). For the strip around x_T the derivatives in x-direction $\partial/\partial x$ for sway in (6.12) are set equal to zero. Furthermore the radiation and diffraction forces and moments in y-direction are also set equal to zero for all sections aft of x_T.

Flow separation also occurs at an immersed transom. Therefore the derivatives $\partial/\partial x$ for heaving in (6.12) are set equal to zero at the transom.
When a ship section, especially a section with a flat bottom, enters the water there is an impact. This doesn't occur when the section is heaving out of the water. In this case the time derivatives for heaving in (6.12) must be set to zero.
All other cases of flow separation are neglected.

6.7 Stability of the Differential Equations

To obtain a stable simulation the complete set of differential equations used for the simulation must be stable. In particular, the set of differential equations used for the calculation of the radiation and diffraction forces must be stable. Due to the large number of these equations and their varying coefficients it seems impossible to test the stability of the set of differential equations as a whole. If one regards the special case of a barge-like ship with constant cross sections, a necessary stability criterion can be formulated. The simulation must be stable for every shape of immersed section area the matrices A and B are calculated for. This means every set of matrices A and B for all the different immersions of the ship sections must be tested for stability. This is no theoretically sufficient criterion for the stability of the simulation, but as experience with the simulation program has shown, it is adequate for practical purposes.
The method for testing the stability of a set of matrices A and B follows.
The differential equation

$$\sum_{k=0}^{kk} D^{k+1}(A_k\,\dot{\underline{u}}_x) = \sum_{k=0}^{kk} D^k(B_k\cdot\underline{f}_x)$$

can for kk = 3 and A_k and B_k being constant be written as

$$F_u = B_0\cdot\underline{f}_x + B_1\cdot D\underline{f}_x + B_2\cdot D^2\underline{f}_x + E\cdot D^3\underline{f}_x \tag{6.43}$$

Here F_u is a function of derivatives of $\dot{\underline{u}}_x$ and B_3 is set equal to the unit matrix E. The equation can be transformed into a system of first order differential equations as follows:

$$D\begin{bmatrix} D^2\underline{f}_x \\ D\underline{f}_x \\ \underline{f}_x \end{bmatrix} = F_u + \begin{bmatrix} -B_2 & -B_1 & -B_0 \\ E & 0 & 0 \\ 0 & E & 0 \end{bmatrix}\cdot\begin{bmatrix} D^2\underline{f}_x \\ D\underline{f}_x \\ \underline{f}_x \end{bmatrix} \tag{6.44}$$

$$\text{or}\quad DF = F_u + C\cdot F$$

The homogeneous equation $DF = C\cdot F$ is stable, if all eigenvalues of C have negative real parts.
A similar approach leads to the equation:

$$F_f = A_0 D\dot{\underline{u}}_x + A_1 D^2\dot{\underline{u}}_x + A_2 D^3\dot{\underline{u}}_x + A_3 D^4\dot{\underline{u}}_x \tag{6.45}$$

where F_f is a function of $\underline{f}_x$ and its derivatives. This equation can also be transformed into several first order differential eqations:

$$D\begin{bmatrix} D^3\dot{\underline{u}}_x \\ D^2\dot{\underline{u}}_x \\ D\dot{\underline{u}}_x \end{bmatrix} = F_f + \begin{bmatrix} -A_3^{-1}\cdot A_2 & -A_3^{-1}\cdot A_1 & -A_3^{-1}\cdot A_o \\ E & 0 & 0 \\ 0 & E & 0 \end{bmatrix} \cdot \begin{bmatrix} D^3\dot{\underline{u}}_x \\ D^2\dot{\underline{u}}_x \\ D\dot{\underline{u}}_x \end{bmatrix} \tag{6.46}$$

$$\text{or} \quad DU = F_f + G \cdot U$$

The homogeneous equation $DU = G\cdot U$ is stable, if all eigenvalues of G have negative real parts.
So for every set of matrices A and B the eigenvalues of C and G have to be calculated and their real parts checked to be negative.

6.8 Force due to Longitudinal Acceleration

The force due to acceleration of the ship in the x-direction is calculated from the product of the added mass m_{11} and the acceleration.
m_{11} is determined by the following empirical formula (from [21]):

$$m_{11} = 2.7\cdot\rho\cdot\nabla\cdot\left(\sqrt[3]{\nabla}/l\right)^2 \tag{6.47}$$

To include this force in the equations of motion, it must be written as a function of the acceleration in the earth coordinate system of, for instance, the origin of the ship coordinate system:

$$f_{la} = -m_{11}\cdot\underline{t}_4^T\cdot\ddot{\underline{\xi}}_o \tag{6.48}$$

With this F_1 is changed to

$$F_1 = \int_l (V_f\cdot\underline{f}_{xa})dx - m_{11}\cdot\begin{bmatrix} t_{11} & t_{21} & t_{31} & 0 & 0 & 0 \\ 0 & 0 & 0 & 0 & 0 & 0 \\ 0 & 0 & 0 & 0 & 0 & 0 \end{bmatrix} \tag{6.49}$$

7 Additional Roll Damping Moment

The matrices A and B used for the calculation of the radiation and diffraction forces contain only part of the total roll damping. Therefore an additional roll damping moment must be added to the forces and moments acting on the ship. It is determined by the following formula:

$$d_{RD} = -b_L \cdot \dot{\varphi} - b_Q \cdot \dot{\varphi} \cdot |\dot{\varphi}| \tag{7.1}$$

$\dot{\varphi}$ is the time derivative of the roll angle (equivalent to ω_ξ).

b_L is a linear, b_Q is a quadratic roll damping coefficient. They are functions of the ship speed and are determined for the natural roll period (they can, for example, be derived from data given in [3]). They should include all roll damping components except for the damping due to wave generation and due to the lift effect caused by the ship's speed. These components are included in the calculation of the radiation and diffraction forces.

8 Longitudinal Resistance

A choice between two methods for calculating the longitudinal resistance is given in the simulation program. The first one uses a resistance coefficient c_R and an exponent p to calculate the resistance according to the formula

$$\underline{f}_{LR} = \begin{pmatrix} c_R \cdot v_x^p \\ 0 \\ 0 \end{pmatrix} \tag{8.1}$$

If this formula seems inadequate, the resistance can be interpolated for the instantaneous speed from a given table of resistance values versus ship speed. The resistance force is assumed to cause no moment around the coordinate centre.
The speed of the ship in the x-direction can be calculated from:

$$v_x = t_4^T \cdot \dot{\underline{\xi}}_O \tag{8.2}$$

9 Transverse Resistance

The transverse resistance force $\underline{f}_T$ and moment $\underline{d}_T$ of the ship can be calculated according to the following formula (from [23]):

$$\begin{pmatrix} \underline{f}_T \\ \underline{d}_T \end{pmatrix} = \int_l -V(x) \cdot \frac{\rho}{2} \cdot v_t \cdot |v_t| \cdot c_D(x) \cdot d \cdot \begin{pmatrix} \cos\varphi \\ -\sin\varphi \\ d/2 \end{pmatrix} dx \qquad (9.1)$$

$V(x)$ is the transformation matrix, defined in (6.29), ρ the density of the sea water, $c_D(x)$ the drag coefficient of the respective section for transverse flow, d the draught, φ the angle of heel.

v_t is the transverse velocity of the respective ship section relative to the water in the η_1-direction, i.e. at right angles to the x-axis and parallel to the mean water surface. It is calculated as follows.

The velocity in the earth coordinate system of a section point is calculated according to equation (2.10), yielding velocities $\dot{\xi}$ and $\dot{\eta}$. With the course angle ψ the velocity in the η_1-direction can be determined from

$$\dot{\eta}_1 = -\dot{\xi} \cdot \sin\psi + \dot{\eta} \cdot \cos\psi \qquad (9.2)$$

If the components of the orbital velocity in ξ- and η-direction are called $\dot{\xi}_{Orb}$ and $\dot{\eta}_{Orb}$ respectively, the transverse velocity v_t of a ship section can be written as

$$v_t = -(\dot{\xi} - \dot{\xi}_{Orb}) \cdot \sin\psi + (\dot{\eta} - \dot{\eta}_{Orb}) \cdot \cos\psi \qquad (9.3)$$

The orbital velocities are calculated at the section centroid, which can be approximated by the point (x, 0, z1-d/2), with z1 = mean section area / mean waterline breadth.

The transverse resistance defined in this way does not include the transverse *lift* force and its moment which are proportional to the product of longitudinal and transverse relative velocity. This lift is included in the *end effects* of the radiation and diffraction forces.

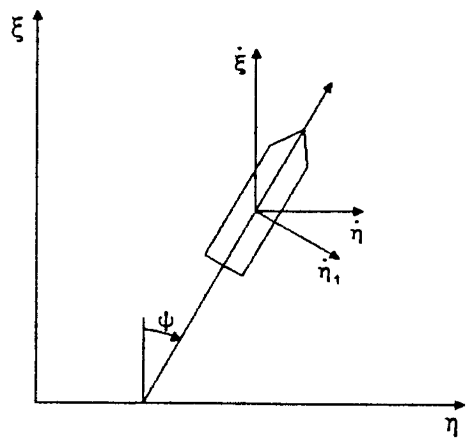

10 Propeller Force and Revolutions

10.1 Force

The propeller force is calculated acording to the formula:

$$\underline{f}_P = \begin{pmatrix} \rho \cdot n^2 \cdot d_p^4 \cdot k_T \cdot (1 - t) \\ 0 \\ 0 \end{pmatrix} \tag{10.1}$$

with:

ρ = density of sea water
n = number of revolutions per time of the propeller
d_p = propeller diameter
k_T = thrust coefficient
t = thrust deduction fraction

The propeller force is assumed to be acting in the x-direction. As with its counterpart, the resistance, no moment around the coordinate centre is taken into account. The thrust coefficient k_T and the torque coefficient k_Q used below are calculated from a polynomial representation of the Wageningen B-series, depending on the number of blades, blade area ratio, pitch and instantaneous advance coefficient of the propeller. The advance coefficient is defined as:

$$j = \frac{v_p}{n \cdot d_p} \tag{10.2}$$

v_p is the x-component of the relative speed of the water with respect to the propeller. It is calculated taking into account the wake fraction and the x-component of the orbital velocity:

$$v_p = v_x \cdot (1 - w) - v_{Orbx} \tag{10.3}$$

v_x is the ship's forward speed (in x-direction, equ. 8.2), w is the wake fraction, v_{Orbx} is the x-component of the orbital velocity at the propeller (the calculation of the orbital velocity is treated in appendix D). w is assumed to be constant.
If there is more than one propeller, the propeller force has to be multiplied by the number of propellers. All propellers are assumed to have equal properties.

10.2 Revolutions

The number of revolutions of the propeller is determined by numerical integration of the differential equation of the propulsion plant (from [23]):

$$\dot{n} = \frac{-\rho \cdot n^2 \cdot d_p^5 \cdot k_Q + d_{pr}(n) \cdot \eta_w}{2 \cdot \pi \cdot j_{pr}} \tag{10.4}$$

k_Q = torque coefficient of propeller acc. to Wageningen B-series
$d_{pr}(n)$ = torque of the propulsion plant as a function of the number of revolutions
η_w = efficiency of shafting arrangement
j_{pr} = polar moment of inertia of the propulsion unit including propeller based on the number of revolutions of the propeller

11 Rudder Forces and Rudder Angle

The calculation of the rudder forces is done as decribed in [24]. Additionally the changing immersion of the rudder in the seaway as well as the orbital velocity at the rudder is taken into account.

11.1 Forces in Ideal Fluid

c_{L1}, the lift coefficient per angle of attack (valid for small angles of attack), is calculated according to the lifting line method described in [24]. In this calculation the extent of the propeller slipstream and the different flow velocities inside and outside of the slipstream are taken into account. From these flow velocities a mean rudder advance velocity in the x-direction v_m is derived. Thus a ratio v_{am} of propeller advance velocity v_a by mean rudder advance velocity v_m can be determined:

$$v_{am} = v_a / v_m \tag{11.1}$$

c_{L1} and v_{am} are calculated in advance for a number of differing values of rudder immersion and propeller advance velocity. During the simulation their actual values are interpolated for the instantaneous rudder immersion and propeller advance velocity. The actual mean rudder advance velocity u_m is then given by:

$$u_m = \frac{-v_p}{v_{am}} \tag{11.2}$$

where v_p is the actual propeller advance velocity as given in (10.3). u_m is positive in the forward direction, so it is normally negative.
The mean flow direction at the rudder relative to the x-axis is calculated acc. to equ. 75 from [24] which is modified to include the y-component of the orbital velocity:

$$\varepsilon = \frac{\omega_z \cdot (x_T - x_R + c/2) - v_{Orby}}{u_m} \tag{11.3}$$

ω_z is the rotational velocity of the ship around the z-axis (relative to the earth coordinate system), x_T is the position of the trailing edge of the ship's hull, x_R is the position of the lift centre of the rudder, and c is the mean chord length of the rudder. v_{Orby} is the y-component of the orbital velocity calculated at the point $(x_R+c/2, 0, z_R)$, with z_R being the z-coordinate of the lift centre of the rudder. It is approximated by the z-coordinate corresponding to half the (vertical) length of the immersed part of the rudder. ω_z is given by:

$$\omega_z = \underline{t}_6^T \cdot \underline{\omega}_\xi \tag{11.4}$$

With the rudder angle δ (positive, if the rudder is turned to port) the effective angle of attack of the rudder is:

$$\alpha = r \cdot \delta + \varepsilon \tag{11.5}$$

r is the ratio between the lift of a flapped rudder with front part assumed to be in the undisturbed flow direction and the lift of an all-movable rudder. This means that $r = 1$ for an all-movable rudder; for rudders with a tail flap r is greater than 1; for rudders with a fixed front part the following equation (equ. 72 from [24]) can be used:

$$r = \frac{(1 + a)\cdot b}{1 + a\cdot b}; \qquad a = 2.93\cdot\left(1 + \frac{0.35}{\lambda}\right)^3 \tag{11.6}$$

b is the ratio of movable area by total area, λ is the aspect ratio of the rudder (defined as (rudder height)^2 divided by rudder area). In the simulation a constant value for r is used.
The lift coefficient of the rudder in ideal fluid is:

$$c_L = c_{L1}\cdot\sin\alpha \tag{11.7}$$

The coefficient of induced drag is:

$$c_D = \frac{c_L^2}{\pi\cdot\lambda} \tag{11.8}$$

Lift and drag are:

$$l = c_L\cdot\rho/2\cdot u_m^2\cdot a_R \tag{11.9}$$

$$d = c_D\cdot\rho/2\cdot u_m^2\cdot a_R \tag{11.10}$$

a_R is the immersed rudder area, ρ is the density of the water.
Force and moment in ideal fluid are:

$$\underline{f}_{RI} = \begin{pmatrix} l\cdot\sin\varepsilon - d\cdot\cos\varepsilon \\ (l\cdot\cos\varepsilon + d\cdot\sin\varepsilon)\cdot(1 + a_H) \\ 0 \end{pmatrix} \tag{11.11}$$

$$\underline{d}_{RI} = \begin{pmatrix} -(l\cdot\cos\varepsilon + d\cdot\sin\varepsilon)\cdot(1 + a_H)\cdot z_R \\ 0 \\ (l\cdot\cos\varepsilon + d\cdot\sin\varepsilon)\cdot(1 + a_H)\cdot(x_R + \Delta x_L) \end{pmatrix} \tag{11.12}$$

a_H is the relative increase of the lift and Δx_L is the forward shift of the centre of lift due to the hull in front of the rudder. Approximate formulae for calculating these values are given in [24]. a_H and Δx_L are calculated in advance for a number of immersions of the rudder and interpolated during the simulation.

11.2 Additional Force in Real Fluid

An additional force is present in real fluid. If v_y is the flow velocity in y-direction at the rudder relative to the ship, then the flow velocity perpendicular to the rudder plane and in starboard direction is:

$$v_q = -u_m\cdot\sin\delta + v_y\cdot\cos\delta \tag{11.13}$$

v_y can be calculated from:

$$v_y = \underline{t}_5^T \cdot (\dot{T} \cdot \underline{x}_r + \dot{\underline{\xi}}_O - \underline{v}_{Orb\xi}) \tag{11.14}$$

where $\underline{x}_r = (x_R, 0, z_R)$ and $\underline{v}_{Orb\xi}$ is the orbital velocity vector at this point.
The resulting force perpendicular to the rudder plane is:

$$f_{rr} = \frac{\rho}{2} \cdot v_q \cdot |v_q| \cdot c_{DR} \cdot a_R \tag{11.15}$$

c_{DR} is the drag coefficient of the rudder in transverse flow. In the simulation a constant value is used for all rudder immersions.

11.3 Total Rudder Forces

The total rudder forces and moments in the ship coordinate system are:

$$\underline{f}_R = \underline{f}_{Ri} + \begin{pmatrix} -f_{rr} \cdot \sin\delta \\ f_{rr} \cdot \cos\delta \\ 0 \end{pmatrix} \tag{11.16}$$

$$\underline{d}_R = \underline{d}_{Ri} + \begin{pmatrix} -z_R \cdot f_{rr} \cdot \cos\delta \\ 0 \\ x_R \cdot f_{rr} \cdot \cos\delta \end{pmatrix} \tag{11.17}$$

11.4 Rudder Angle, Auto Pilot

The rudder angle is determined by the following differential equation, which is used to simulate an auto-pilot:

$$\dot{\delta} = c_1 \cdot (\psi - \psi_c) + c_2 \cdot \dot{\psi} + c_3 \cdot \ddot{\psi} \tag{11.18}$$

δ is the rudder angle, ψ is the yaw angle, ψ_c is the course to be steered. The characteristics of the auto-pilot are determined by the constants c_1, c_2, and c_3. The choice of these constants depends on the manœuvring characteristics of the ship and the environmental conditions (seaway, wind, etc.).

12 Wind Forces

Wind Forces are calculated according to Wagner [25].
The wind force is given by:

$$\underline{f}_w = \frac{\rho_L}{2} \cdot v_{rw}^2 \cdot \begin{pmatrix} c_{x(Ax)} \cdot a_x \\ c_Y \cdot a_L \\ 0 \end{pmatrix} \tag{12.1}$$

The moment due to the wind is given by:

$$\underline{d}_w = \frac{\rho_L}{2} \cdot v_{rw}^2 \cdot a_L \cdot \begin{pmatrix} c_K \cdot h_{Lm} \\ 0 \\ c_N \cdot L_{oa} \end{pmatrix} \tag{12.2}$$

In these equations the following symbols were used:

a_L	area of the lateral projection of the ship above the waterline
a_x	projected area of the ship above the waterline as seen from forward
$c_{x(Ax)}$	coefficient for the longitudinal force based on a_x
c_Y	coefficient for the transverse force
c_K	coefficient for the rolling moment
c_N	coefficient for the yaw moment
ρ_L	density of air
v_{rw}	wind velocity relative to the ship
L_{oa}	overall length of the ship
h_{Lm}	a_L / L_{oa}

The coefficients c depend on the shape of the ship above the water surface and are functions of the angle of attack ε_w. They can be determined by wind tunnel experiments or taken from [25] for similar ship shapes.
The relative wind velocity v_{rw} is the result of the vector addition of the negative forward speed of the ship v_S and the wind velocity v_w.
For a heeled ship the force in y-direction and the moments around the x- and z-axis must be modified. If the ship is heeling towards the side the wind is coming from, no modification is made. If it is heeling in the other direction, the force and moments are multiplied by the factor

$$0.25 + 0.75 \cdot (\cos\varphi)^3 \tag{12.3}$$

given in [21]. φ is the heel angle.

During the course of the development of the simulation method presented in this paper a new, much more refined method for calculating wind forces has been published [2], which may be used in the future to replace the procedure described here.

13 Total Forces and Moments

The following components of the forces and moments acting on the ship are considered in the simulation model:

Forces due to the ship's weight	$\underline{f}_g$, $\underline{d}_g$
Froude-Krilov-Forces	$\underline{f}_F$, $\underline{d}_F$
Radiation and diffraction Forces	
Additional Roll Damping Moment	$\underline{d}_{RD}$
Longitudinal resistance	$\underline{f}_{LR}$
Transverse resistance	$\underline{f}_T$, $\underline{d}_T$
Propeller force	$\underline{f}_P$
Rudder forces	$\underline{f}_R$, $\underline{d}_R$
Wind forces	$\underline{f}_W$, $\underline{d}_W$

Those force and moment components which are functions of the accelerations must be treated seperately from all other forces as shown in equations 3.9 and 3.10. Of the forces listed above, the radiation and diffraction forces have components, which are functions of the acceleration. They are included in the matrices F_1 and D_1 given in chapter 6.
All other forces and moments do not depend on any accelerations and can be added to form the vectors $\underline{f}_2$ and $\underline{d}_2$ given in (6.41) and (6.42). The forces $\underline{f}_{other}$ and moments $\underline{d}_{other}$ are expressed by the following sums:

$$\underline{f}_{other} = \underline{f}_g + \underline{f}_F + \underline{f}_{LR} + \underline{f}_T + \underline{f}_P + \underline{f}_R + \underline{f}_W$$

$$\underline{d}_{other} = \underline{d}_g + \underline{d}_F + \underline{d}_{RD} + \underline{d}_T + \underline{d}_R + \underline{d}_W$$

Other forces acting on the ship can be easily included in these equations, as long as they are independent of accelerations.

14 Comparison With Strip Method Results

For the comparison with the strip method simulations were done in head waves of different wave lengths for a container ship (ship A, which was also used in capsizing model experiments in the HSVA; the particulars of the ship are given in appendix E). Since the strip method is a linear method, small wave amplitudes (0.1m) had to be chosen for the comparison to exclude non-linear effects in the simulation. The simulations were terminated when the ship's oscillations had become stable for several periods. Figure 14-1 shows an example of the results of such a simulation run (motions plotted over time). In the simulation program numbers are represented with an accuracy of seven digits. Due to this limited accuracy the wave angle is not exactly equal to the number π. This leads to the very small motions for yaw, roll, and sway shown in figure 14-1.
Transfer functions for heave and pitch were calculated from the motion amplitudes. The transfer function for heave is defined as

$$Y_{\zeta} = \frac{\zeta_{max} - \zeta_{min}}{2 \cdot \zeta_A}$$

ζ_{max} and ζ_{min} are the maximum and minimum heave motion respectively, ζ_A is the wave amplitude.
The transfer function for pitch is defined as

$$Y_{\vartheta} = \frac{\vartheta_{max} - \vartheta_{min}}{2 \cdot \zeta_A \cdot k}$$

ϑ_{max} and ϑ_{min} are the maximum and minimum pitch angle respectively, k is the wave number.
Figures 14-2 to 14-5 show a comparison of the transfer functions for heave and pitch for ship A at two different forward speeds with the results obtained by strip theory. Agreement is very good.
Simulations were also done for larger wave amplitudes. Figures 14-6 and 14-7 show a comparison of transfer functions for wave amplitudes 0.1m and 3.0m. A significant difference due to non-linear effects can be seen in the frequency range from $0.4 s^{-1}$ to $0.6 s^{-1}$ (corresponding to ratios of wave length by ship length of 2.85 to 1.27)

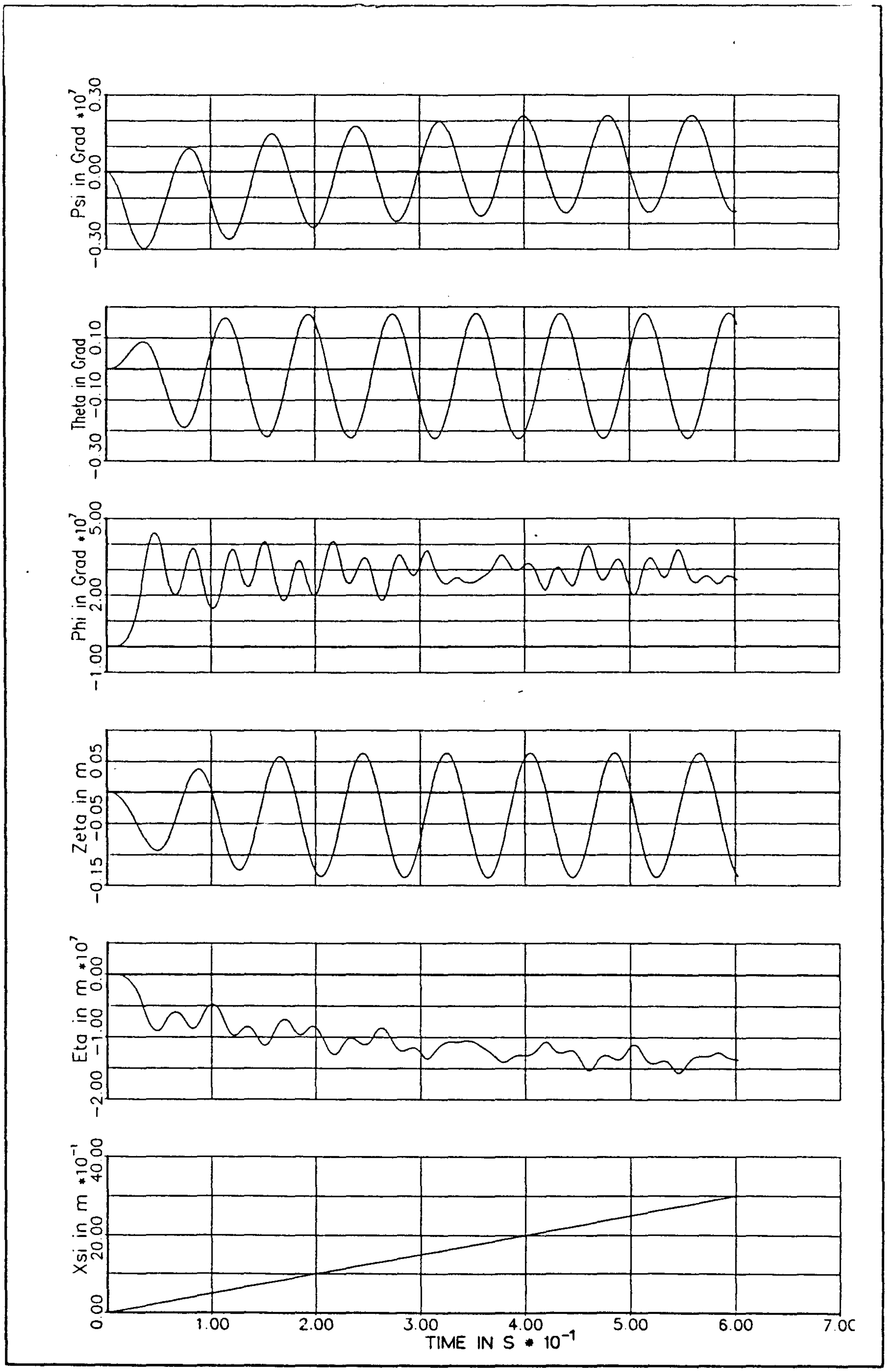

Figure 14-1: Simulation in regular head wave, amplitude 0.1m, circ. freq. $0.6s^{-1}$, ship speed 9m/s

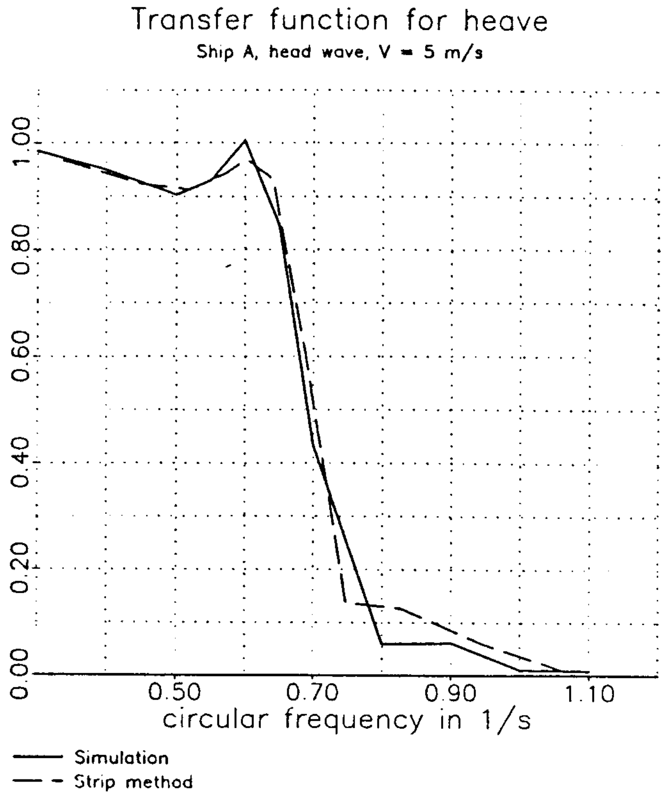

Figure 14-2: Transfer function for heave, head wave, v = 5 m/s

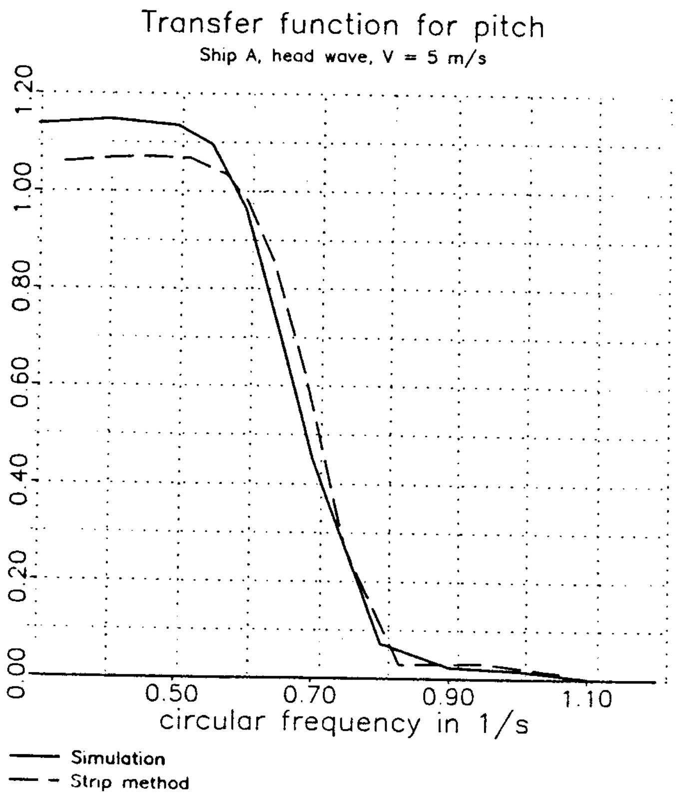

Figure 14-3: Transfer function for pitch, head wave, v = 5 m/s

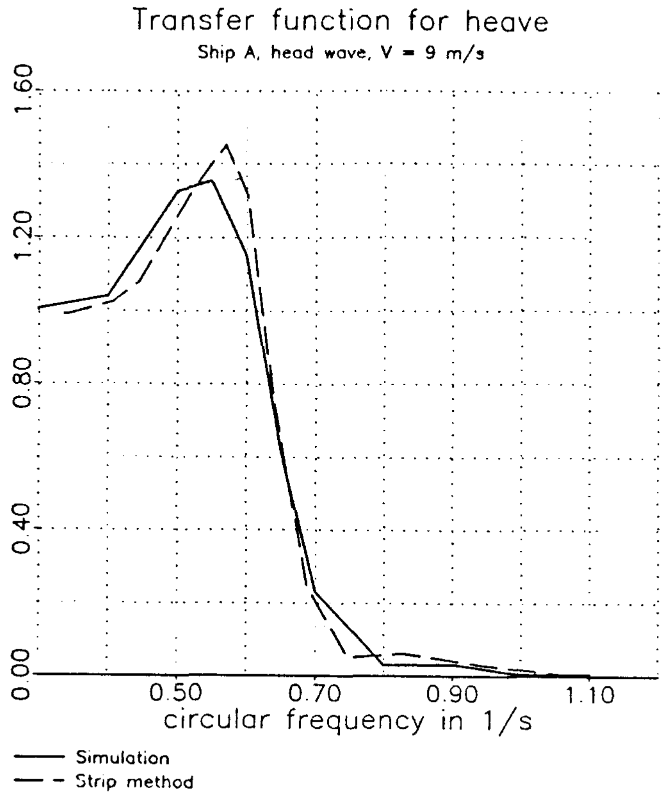

Figure 14-4: Transfer function for heave, head wave, v = 9 m/s

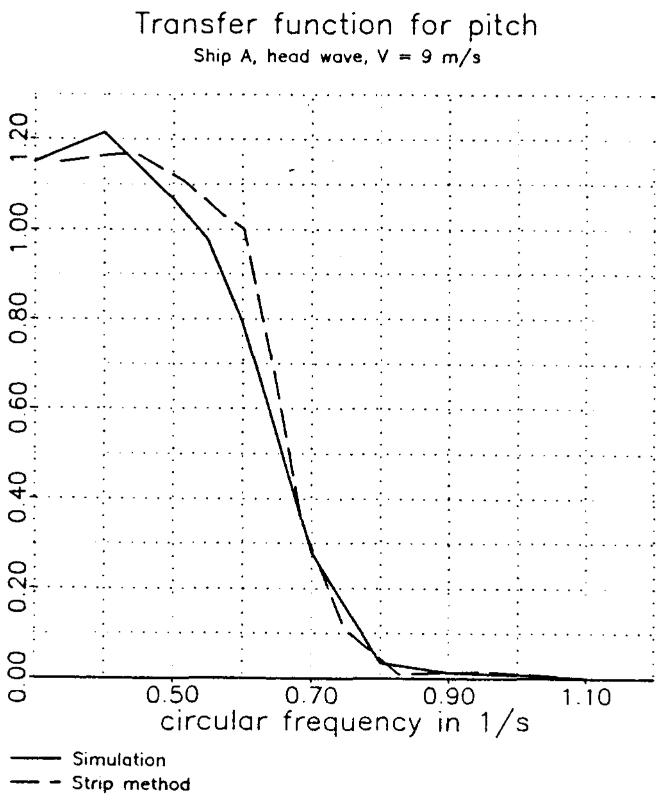

Figure 14-5: Transfer function for pitch, head wave, v = 9 m/s

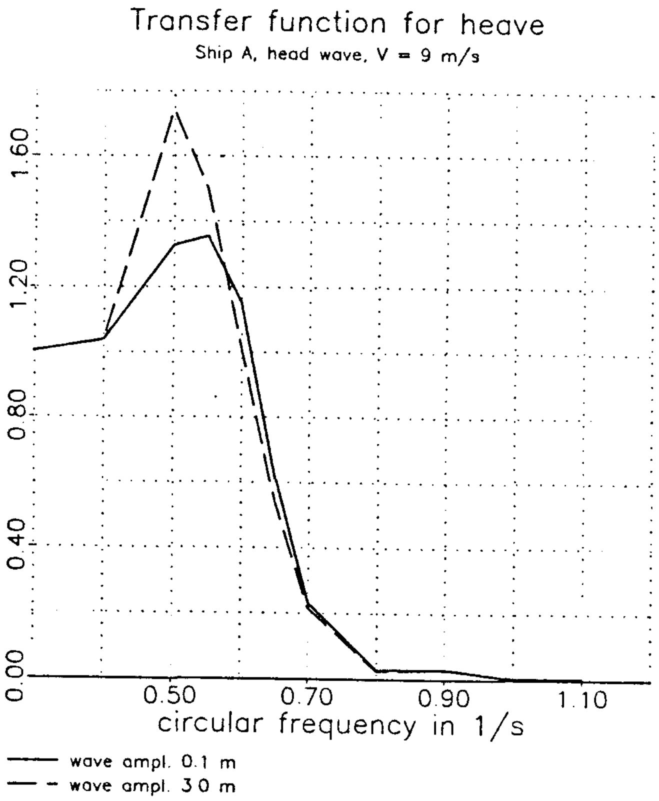

Figure 14-6: Transfer function for heave, head wave, v = 9 m/s

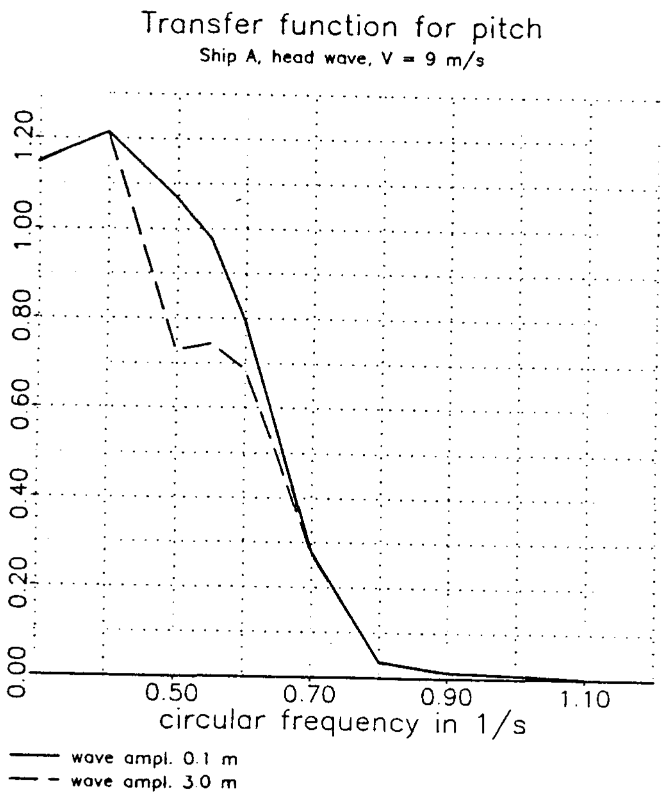

Figure 14-7: Transfer function for pitch, head wave, v = 9 m/s

15 Comparison With Experiments

15.1 Introduction

In the years 1982 to 1986 an investigation into the intact stability of container ships was made in the HSVA [4, 5]. For this purpose four container ship models named A to D were tested in regular and irregular waves. The experiments in regular waves were performed for one metacentric height only, but with different static heeling moments. The tests in irregular waves were done for different metacentric heights to find limiting GM values for safety against capsizing.
To assess the applicability of the simulation method presented in this paper for capsizing investigations, simulations were done for model A and compared with the experimental results of the HSVA [5]. The particulars of ship A are listed in appendix E.

15.2 Tests in Regular Waves

15.2.1 Model Tests

The HSVA tests with model A in regular waves were performed for the following condition of the ship:

Draught	8.2 m
GM	1.5 m
Natural period of roll	14.2 s

The wave length was equal to the ship's length (135 m) and the wave height was 9 m (ratio of wave length by wave height: 15), wave direction was from aft. Test runs were done for static heel angles of 5°, 6.9°, 7.8°, and 10.0° to starboard. Figure 15-1, which was taken from [5], shows the maximum roll angles as functions of the mean ship speed. Triangles indicate a capsizing. Lines connecting a symbol and a triangle indicate a capsizing that occurred after a longer nearly stable phase. Two symbols connected by a line indicate cases, where alternating small and large roll amplitudes were observed.

15.2.2 Simulation

Simulation runs were done for the same conditions for static heel angles of 5° and 7.8°. These angles were achieved by shifting the centre of gravity by an appropriate amount in y-direction (table 15-1). In each case a simulation run was done in still water to check the resulting heel angle.

Table 15-1

Heel angle in °	y_G in m
5.0	0.131
7.8	0.212

Table 15-2

KG	8.37 m
I_{Gx}	1098000 tm^2
m	17275 t
x_G	-1.22 m
ρ	1.025 t/m^3

In the model experiments the rudder of the ship was replaced by a rudder of nearly double the area to improve course stability. As in the experiments keeping the ship on course was very difficult in the simulation. Therefore the effectiveness of the rudder was doubled by multiplying the rudder forces and moments by two. A large number of simulation test runs were required for establishing suitable constants for the auto-pilot. Even so it was impossible to keep the ship on course at low forward speeds, which is due to the waning effectiveness of the rudder. Therefore only results for high ship speeds between Fn = 0.22 and 0.263 can be given here.

As can be seen in the simulation results, roll angles tended to be small as long as yaw angles could be kept small. Larger yaw angles lead to larger roll angles, which in turn caused increasing yaw moments due to the resulting asymmetry of the submerged part of the hull.

15.2.3 Static Heel Angle 5°

Figures 15-2 and 15-3 show simulation results for a static heel angle of 5° using different coefficients for the autopilot. In Figure 15-2 the mean ship speed is approximately 9 m/s (Fn = 0.247), the mean roll amplitudes are about 8° to starboard and 2° to port. The maximum roll angle is 12.6°.

In Figure 15-3 the mean speed is approximately 8.5 m/s (Fn = 0.234). The mean roll amplitudes are 10.8° to starboard and 2° to port. The maximum roll angle is 14.1°. In the time range from 500s onwards every three periods there are smaller amplitudes of approximately 7°.

In comparison the roll amplitudes in the model experiments alternated between 7.8° and 12.1° for Fn = 0.263 (Figure 15-1). This agrees quite well with the simulation results shown in figure 15-3.

15.2.4 Static Heel Angle 7.8°

Figures 15-4 to 15-6 show simulation results for a static heel angle of 7.8° to starboard using different auto-pilot constants. In each case a capsize to starboard occurred when the ship could not be held on course and yawed to port. As long as the yaw angles were small, roll amplitudes were in the range of 15° to 20° with peaks of about 28°. The mean forward speed was between 8 m/s (Fn = 0.22) and 10.3 m/s (Fn = 0.28).

As can be seen in figure 15-1 the ship also capsized in the model tests for speeds greater than Fn = 0.22. The capsizes occurred after a long nearly stable phase with roll amplitudes of 30° to 32° (for Fn < 0.29). This is a behaviour similiar to that in the simulation although the roll amplitudes are larger.

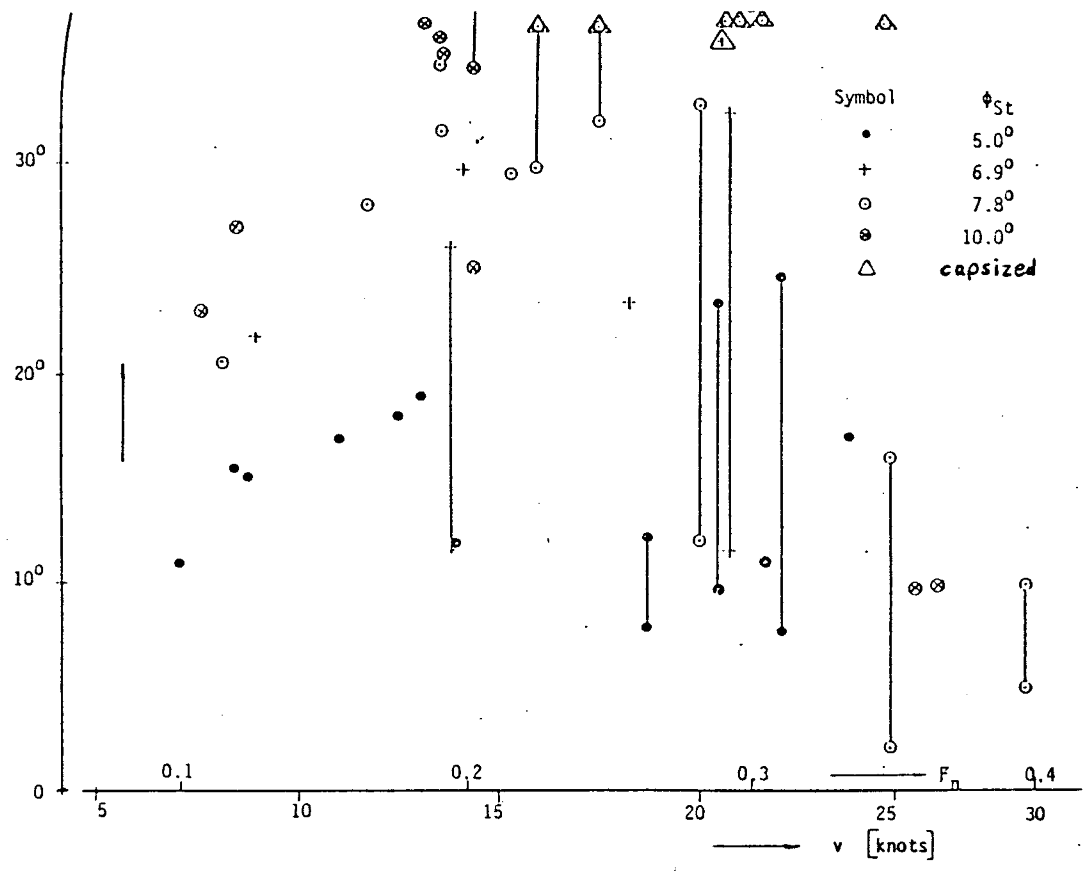

Figure 15-1: Maximum roll angles as a function of the mean speed for 4 static heel angles (experiments in regular waves, from [5]).

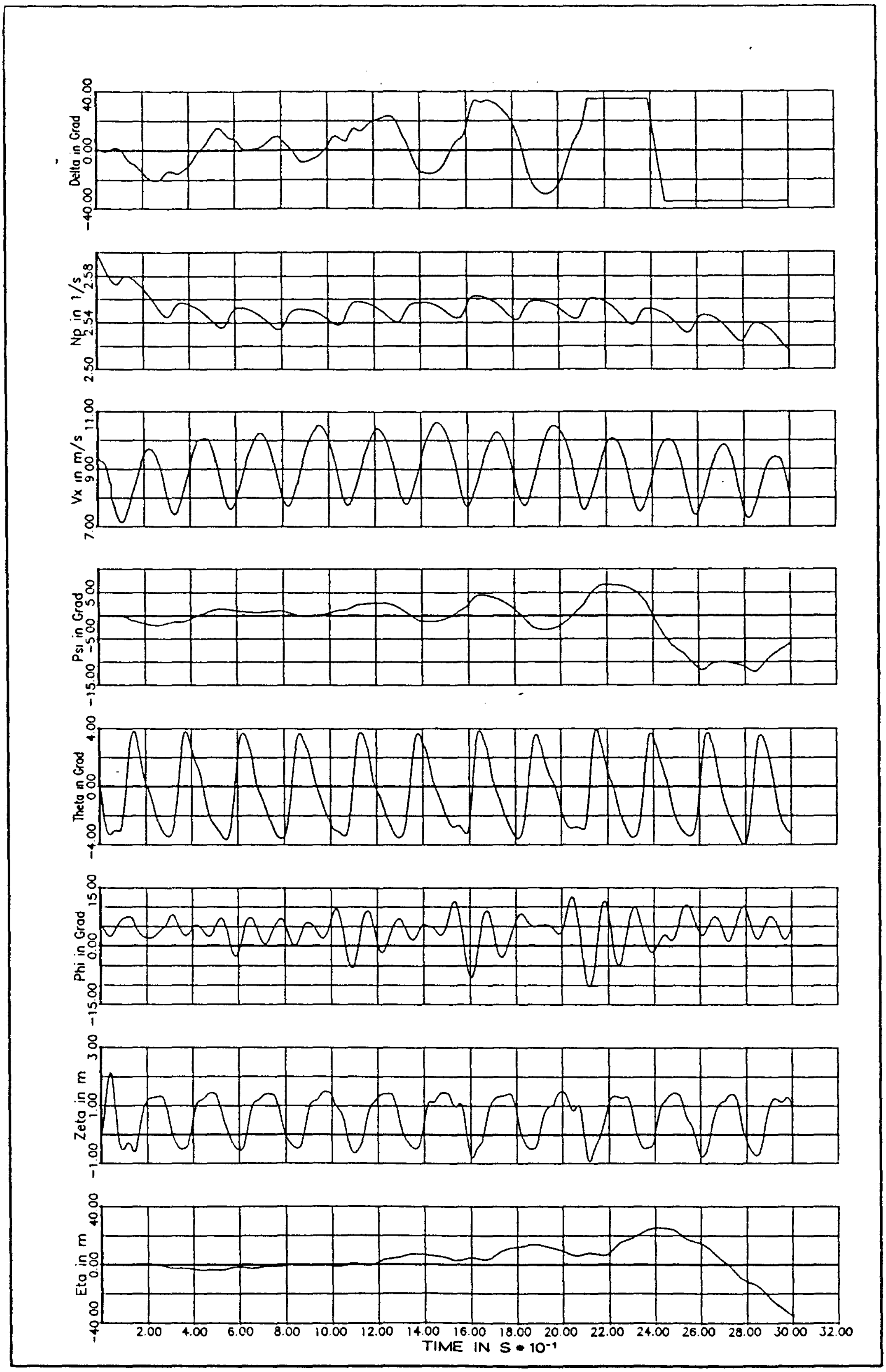

Figure 15-2: Simulation in regular wave, static heel angle 5°, wave height 9m, wave direction 0°, wave length 135m

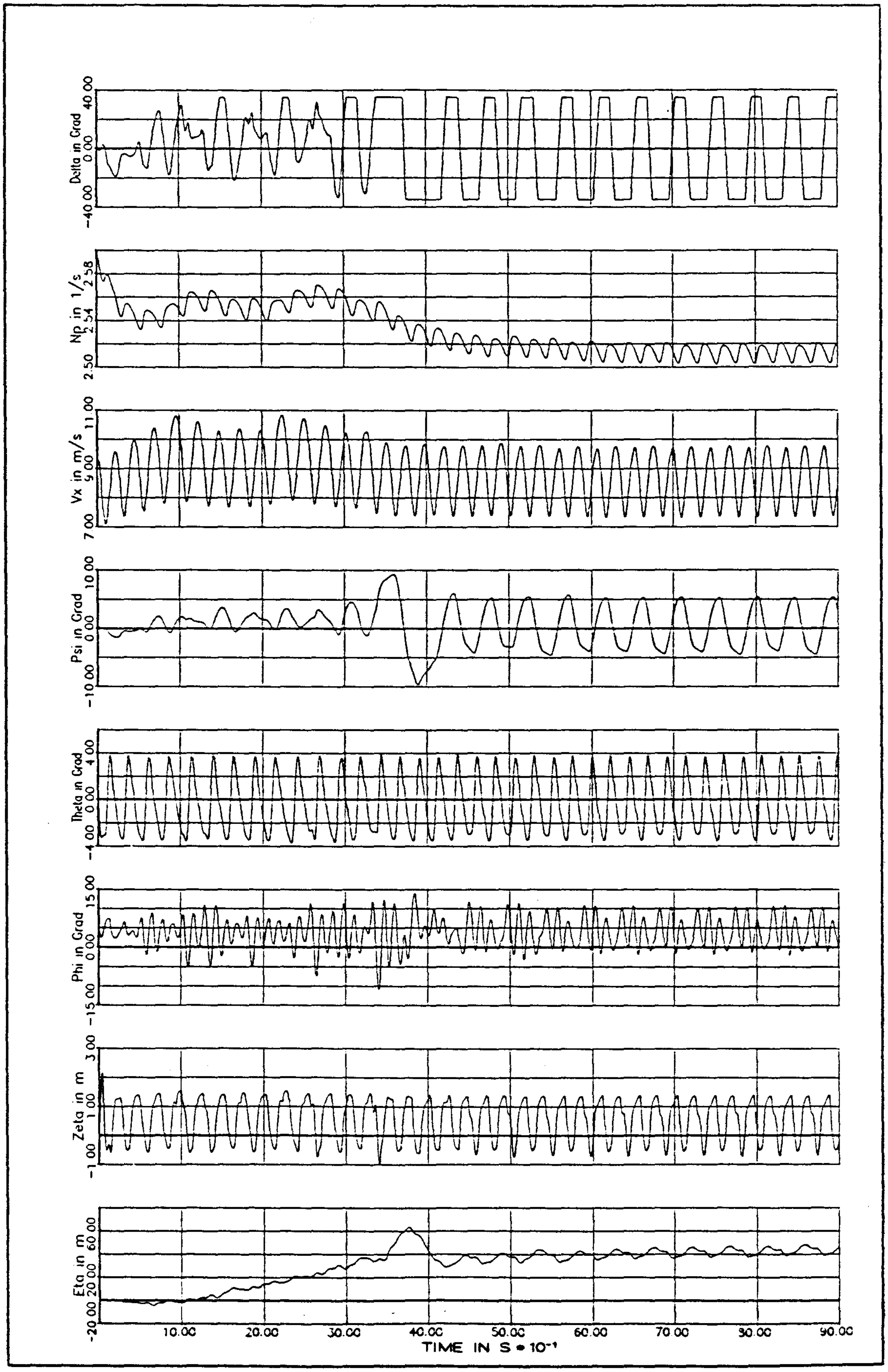

Figure 15-3: Simulation in regular wave, static heel angle 5 , wave height 9m, wave direction 0°, wave length 135m

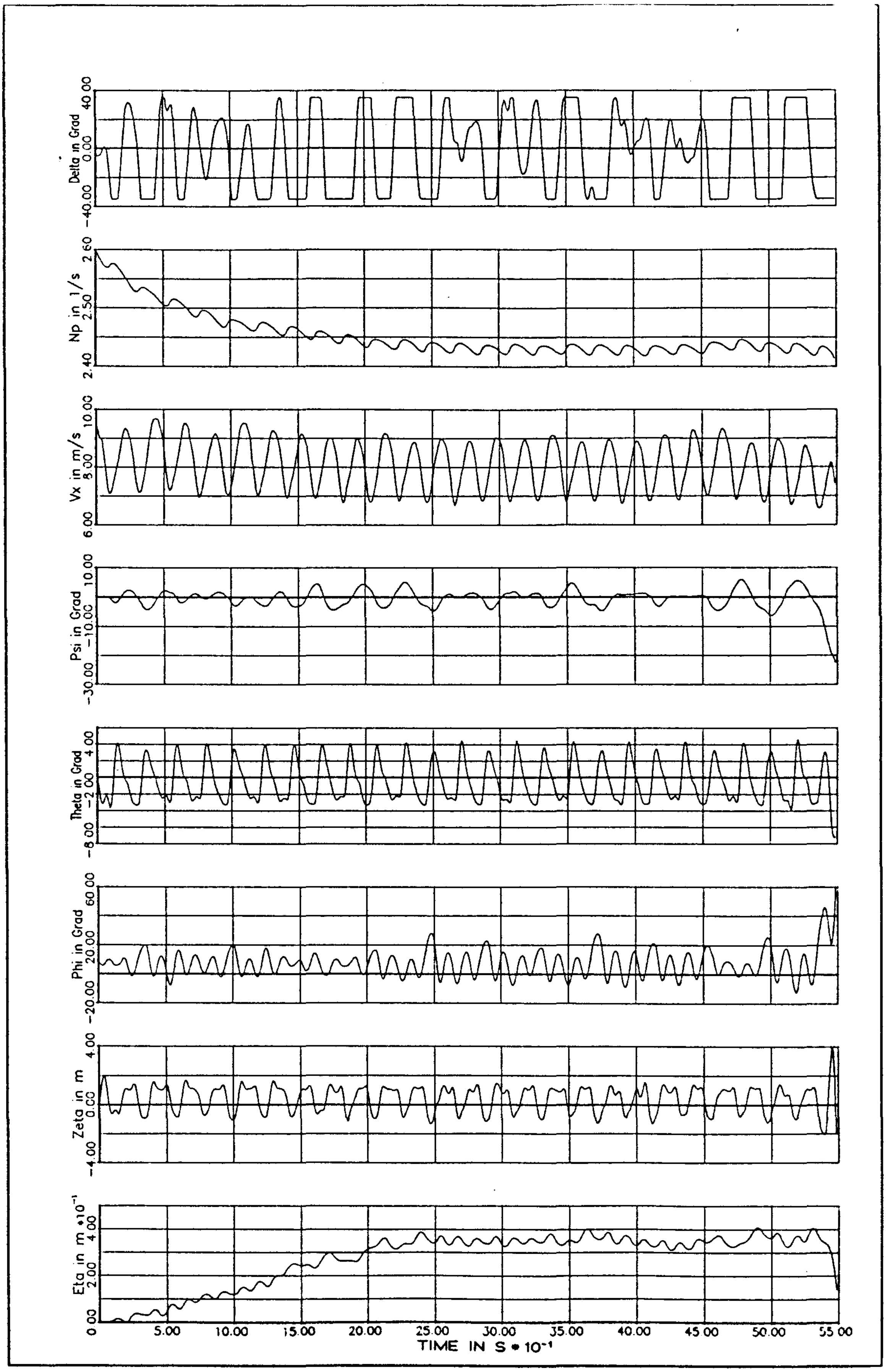

Figure 15-4: Simulation in regular wave, static heel angle 7.8°, wave height 9m, wave direction 0°, wave length 135m

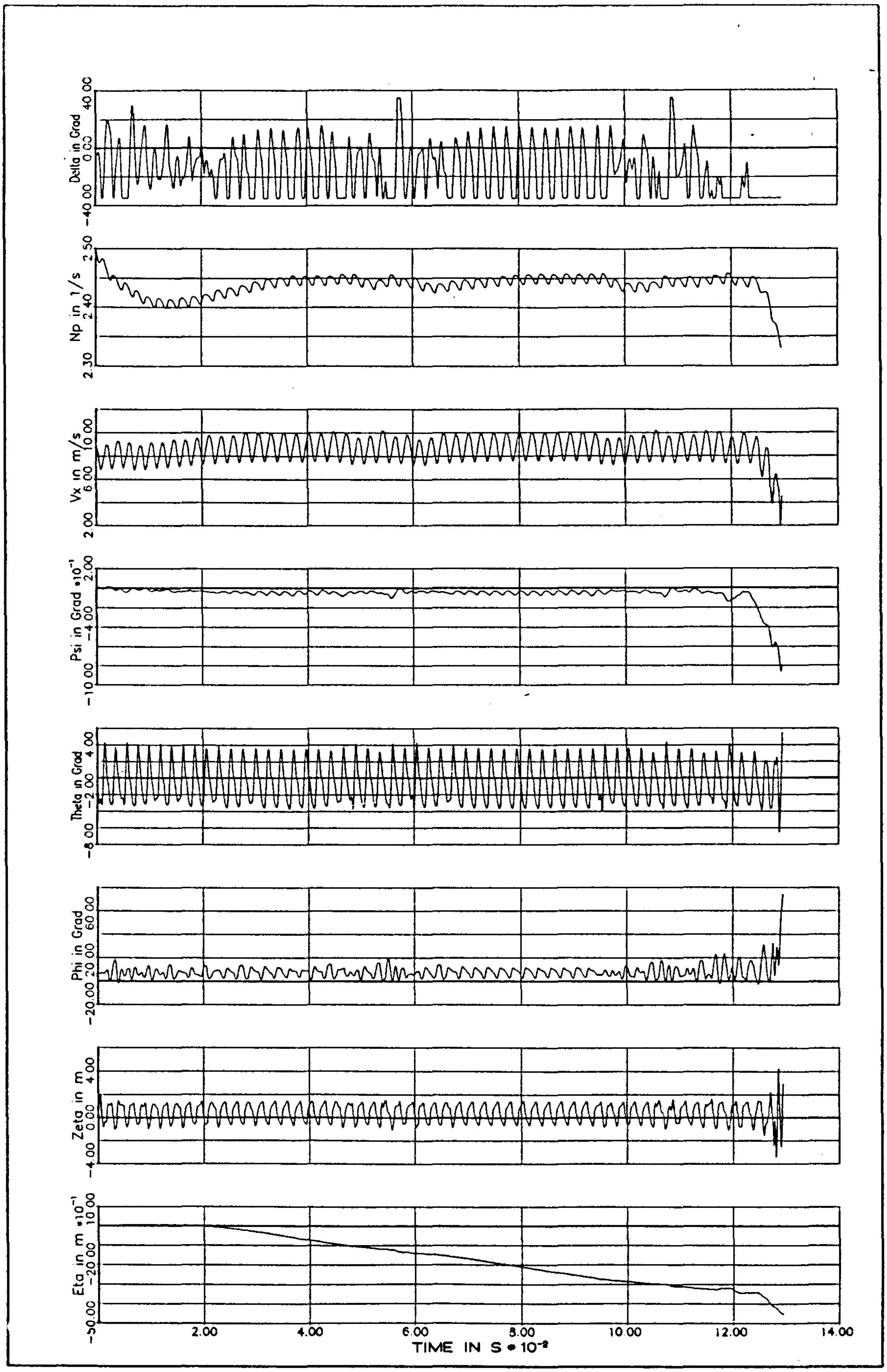

Figure 15-5: Simulation in regular wave, static heel angle 7.8°, wave height 9m, wave direction 0°, wave length 135m

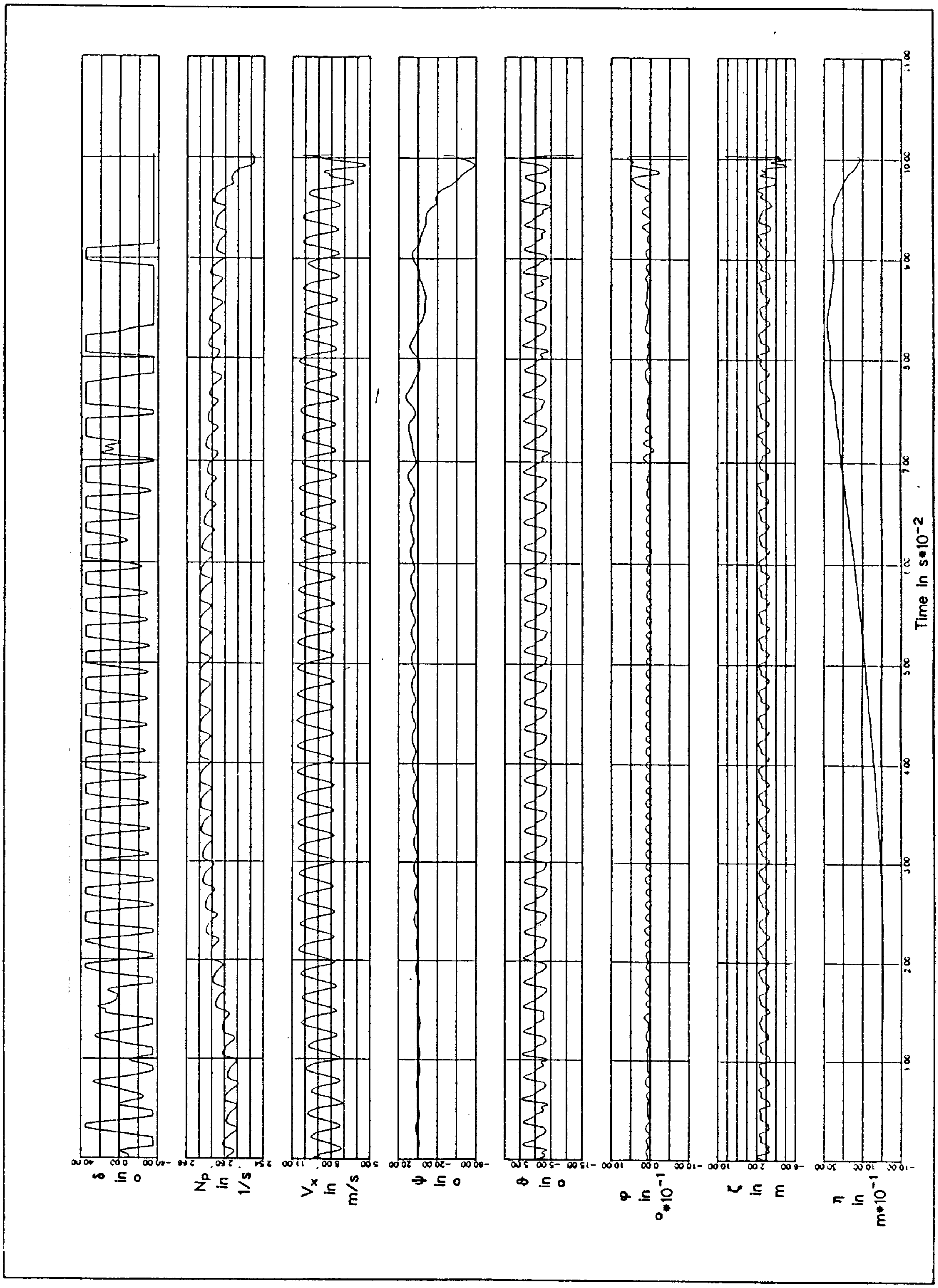

Figure 15-6:. Simulation in regular wave, static heel angle 7.8°, wave height 9m, wave direction 0°, wave length 135m

15.3 Tests in Irregular Waves

15.3.1 Model Tests

The HSVA model tests in irregular seas were performed for three draughts and various metacentric heights in following and beam seas. The seaway had a modal period of 13.1s and a significant wave height of 14.6m. Figure 15-7 (taken from [5]) shows the spectrum of the model seaway compared to the JONSWAP-spectrum. The model seaway was, of course, long crested, since short crested seaways cannot be created in the HSVA tank.

Due to the limited length of the tank the test runs could not be very long. A possibly very improbable event as capsizing might not occur during tests in a seaway closely modelled to reality. Therefore a very severe seaway was chosen. Additionally the test runs were done only in particularly high wave groups. A static heeling moment of 8740kNm was exerted on the model to simulate stationary wind pressure. Gusts were simulated by increasing the heeling moment to 16460kNm in 8.5s and then decreasing it to 8740kNm again.

The aim of the tests was to find a value for the metacentric height GM_O, above which the ship could be regarded as safe against capsizing. For the draught of 8.2m this limiting value was found to be GM_O = 1.70m, although it is suggested in [5] that this value may still be too small.

For an angle of encounter of 0° (directly from aft) 5 test runs were done for GM_O=1.21m with no capsize, 6 test runs were done for GM_O=1.43m and a capsize occured in one of these, 14 test runs were done for GM_O=1.71m with no capsize.

A short description of the tests for GM_O=1.71m is cited here (translated from [5]):

"At this relatively large initial stability (GM_O= 1.71m!) very large heeling angles occurred, when the model was moving in waves of high energy, in conjunction with a large course deviation (...). The heel became particularly large in a case, where in high waves a course deviation of about 10° was levelled off by contrary rudder action (...). In some waves the model was pushed along by a wave crest coming up from aft. In these cases the occuring heel angles were relatively small (< 10°)."

The tests with GM_O=1.43m are described as follows (translated from [5]):

"Of a total of 6 runs the model could be kept in the region of highest, breaking waves. Here very large roll and yaw motions with partly extremely large heeling angles occured. The model was in very large danger of capsizing and in one case capsized to port (with a preset wind heeling to port)."

15.3.2 Simulation

A different approach than that used in the model experiments was used for the simulation. Since the waves and the ship motion could not be observed during the simulation, the ship could not be directed into the particularly high wave groups.

Simulation runs were done for a draught of 8.2m in a seaway with the same spectrum as used in the model experiments. 3 representations of the seaway using component waves with random phase angles were chosen (see appendix F for details). The same static heeling moment (8740 kNm) to the starboard side as in the model experiments was used for simulating wind pressure. Wind gusts were not simulated. Simulations were done for GM_O values of 1.43m, 1.71m, 1.85m, and 2.14m. Average ship speeds were between 9 and 11m/s.

The simulation results are given in figures 15-7 to 15-18. For GM_O=1.43m and wave set 2 (fig. 15-8), GM_O=1.71 and wave set 2 (fig. 15-11), GM_O=1.85m and wave set 1 and 2 (fig. 15-13, 15-14), and GM_O=2.14m and wave set 1 (fig. 15-16) the simulation failed. This means the program terminated abnormally due to impossible internal data (for instance in fig. 15-11 it can be seen that the ship is lifted completely out of the water).There are two possible reasons for this. The starting values for some of the simulation variables, especially the state variables used for calculating the radiation and diffraction forces, were chosen arbitrarily. Therefore a certain simulation time is needed for the influence of these initial values to die out. This time depends largely on the motion damping. Since the damping for the rolling motion isn't large, a long time is needed for the rolling motion to stabilize itself. Another reason could lie in the selection of the wave components for the irregular seaway. It may be possible that the waves of highest energy have a frequency causing instant roll resonance and capsizing.
In the cases of GM_O=1.43m and wave sets 1 and 2 (fig. 15-7, 15-8), GM_O=1.71m and wave set 3 (fig. 15-12), GM_O=2.14m and wave set 3 (fig. 15-18) capsizes occurred. Except for one case (GM_O=1.43m, wave set 1) the capsizes were always coupled with a large course deviation.
The ship didn't capsize in the preset simulation time in the cases of GM_O=1.71m and wave set 1, GM_O=1.85m and wave set 3, GM_O=2.14m and wave set 2. Here the yaw angles were very low.
Generally the ship's behaviour in the simulation is well described by the citations from [5] for the model experiments. However, according to the model experiments the ship shouldn't have capsized in any of the simulation runs for metacentric heights greater than 1.7m. The difference may be due to the higher ship speeds used in the simulation or it may have something to do with the larger inability to keep course observed in the simulation. This may make the ship more prone to broaching to, causing the ship to capsize as a result. There are a number of possible reasons for this. The constants for the autopilot may have been chosen unfavourably. It may also be considered a general weakness that they are constant for the whole simulation run and cannot be adapted or adapt themselves to the actual conditions. It is also generally questionable whether any kind of auto-pilot can be used to good effect in extreme sea states, particularly in following waves where the rudder effectiveness is very low.
Another possible reason for the greater course deviations in the simulation can lie in the selection of the drag coefficients for the transverse resistance (due to lack of data they were set to 1.0 for all sections).
The longitudinal motion also appears problematic. The changes in the forward speed seem to be very large, which made the adjustment of the speed very difficult. Unfortunately the variations in speed cannot be compared with the experiments since such data are not given in the report on the model tests [5].

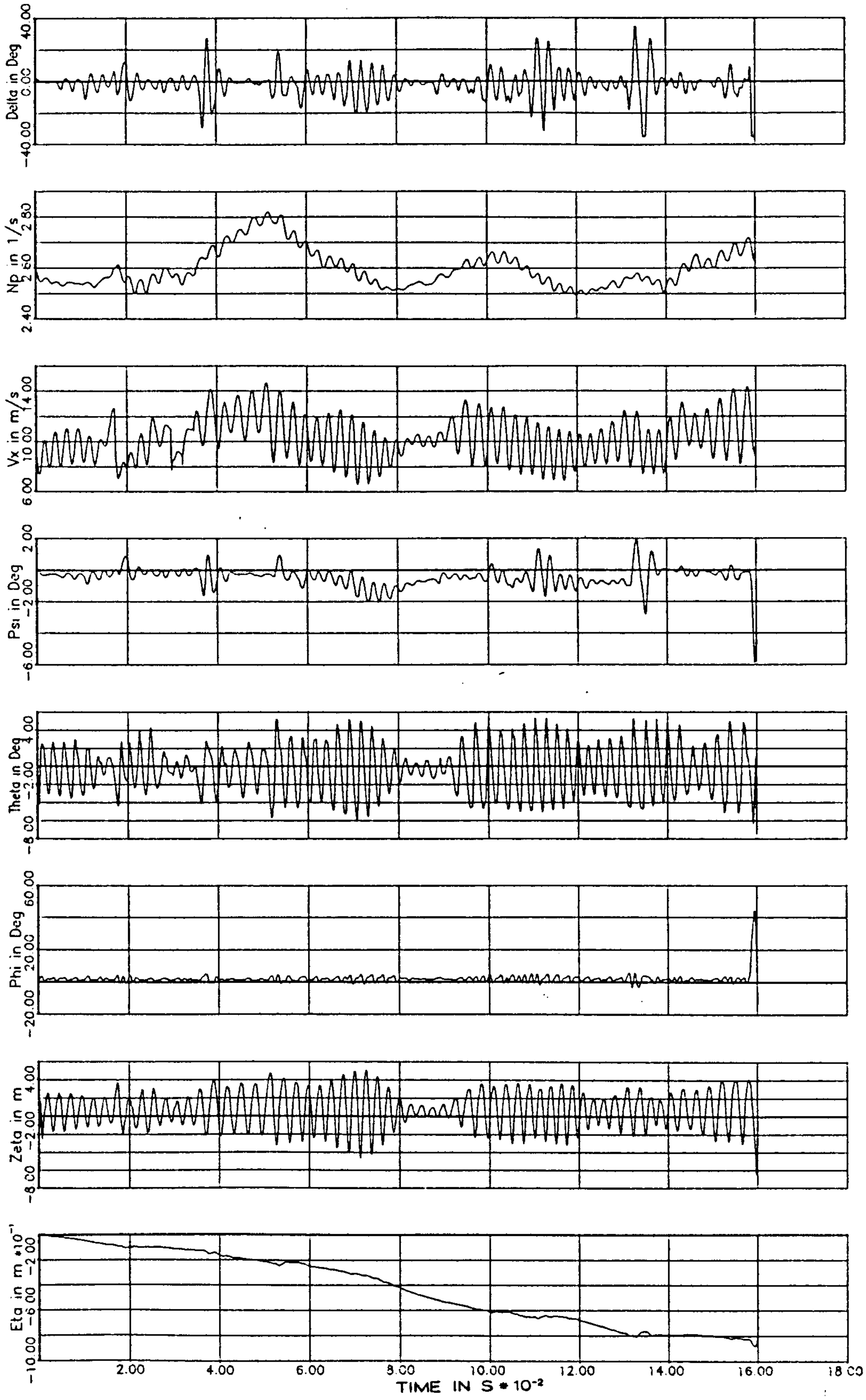

Figure 15-7: Simulation in irregular seaway, wave set 1, GM_O=1.43m

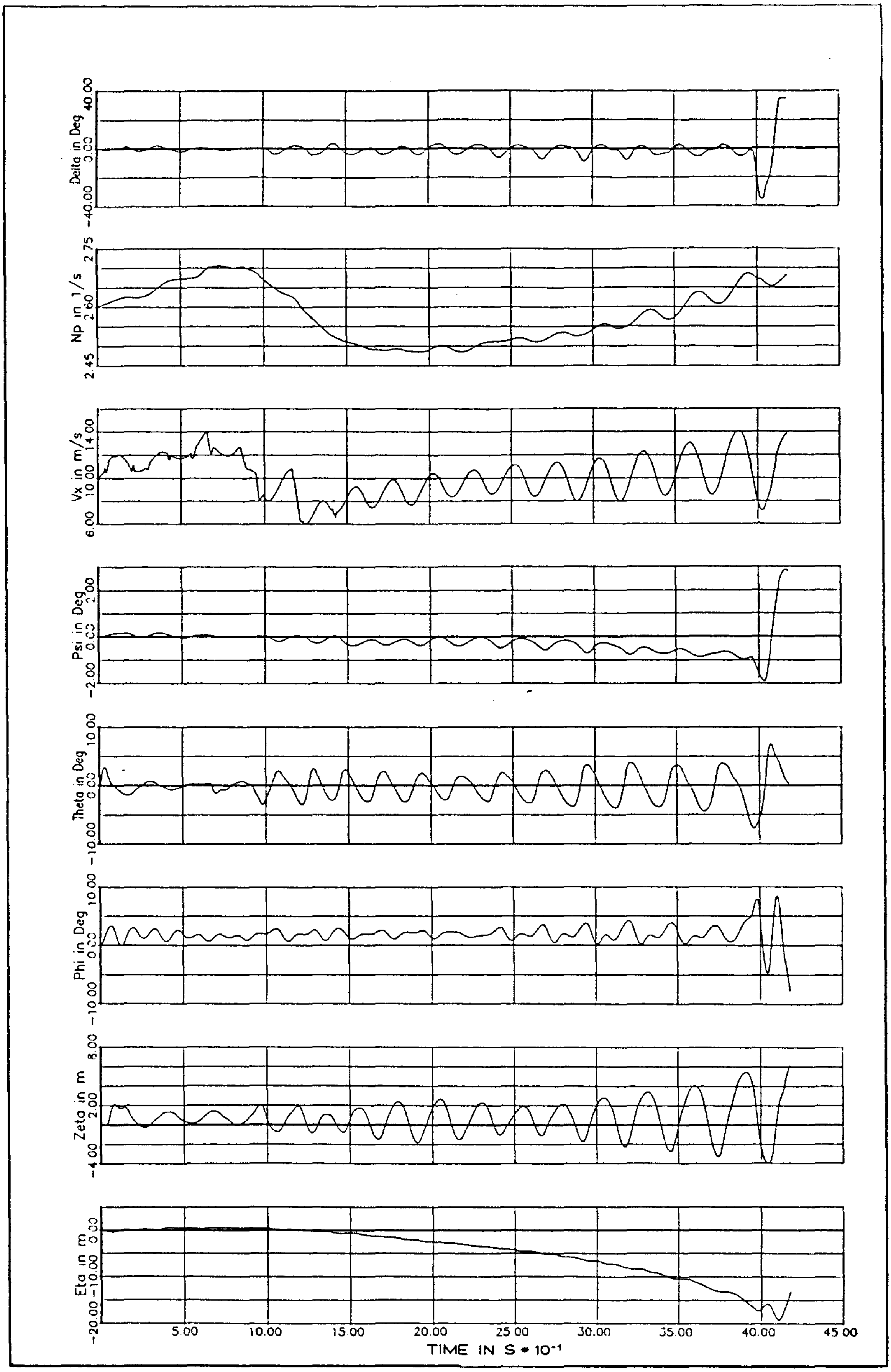

Figure 15-8: Simulation in irregular seaway, wave set 2, GM_O=1.43m

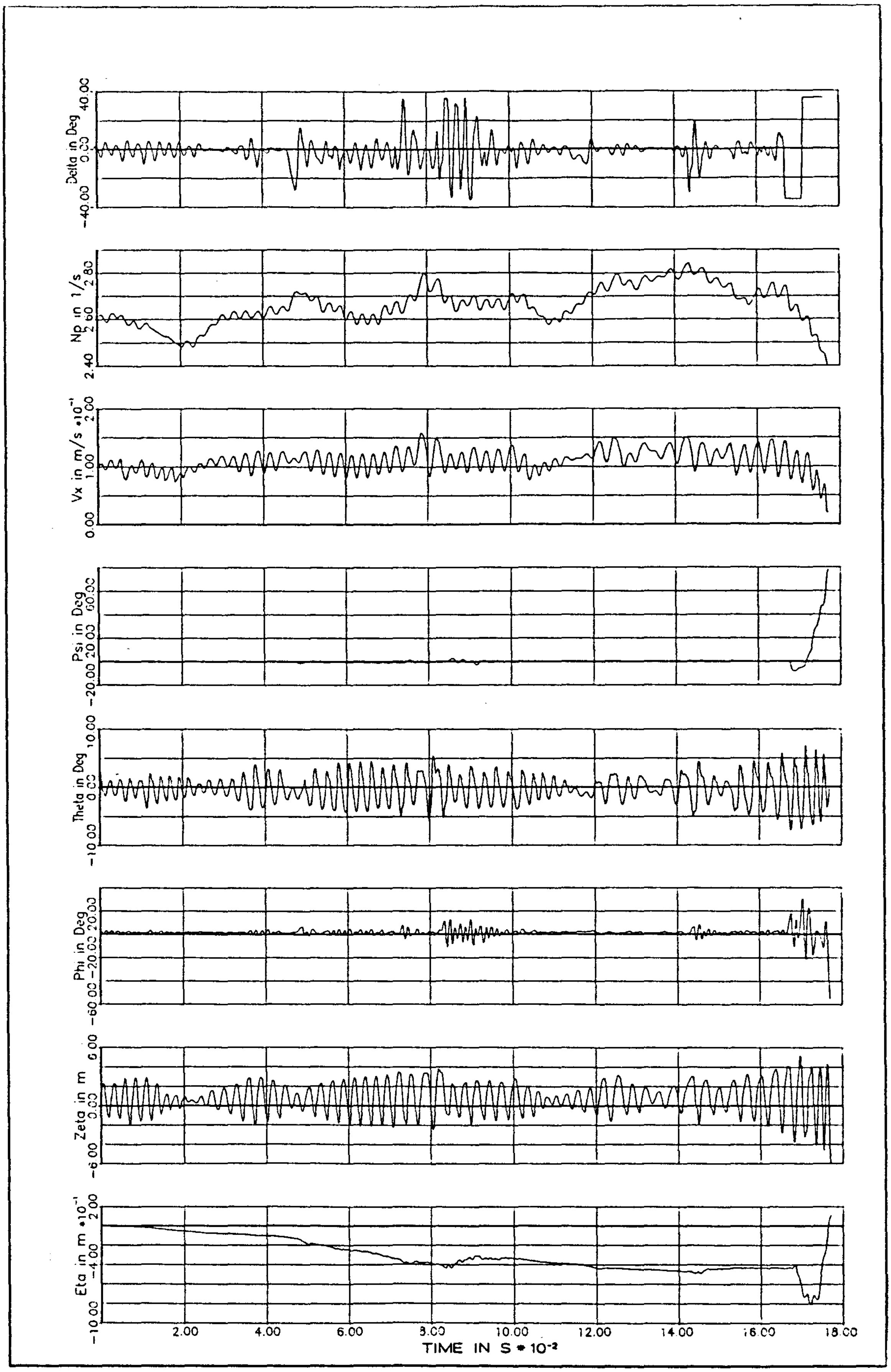

Figure 15-9: Simulation in irregular seaway, wave set 3, GM_0=1.43m

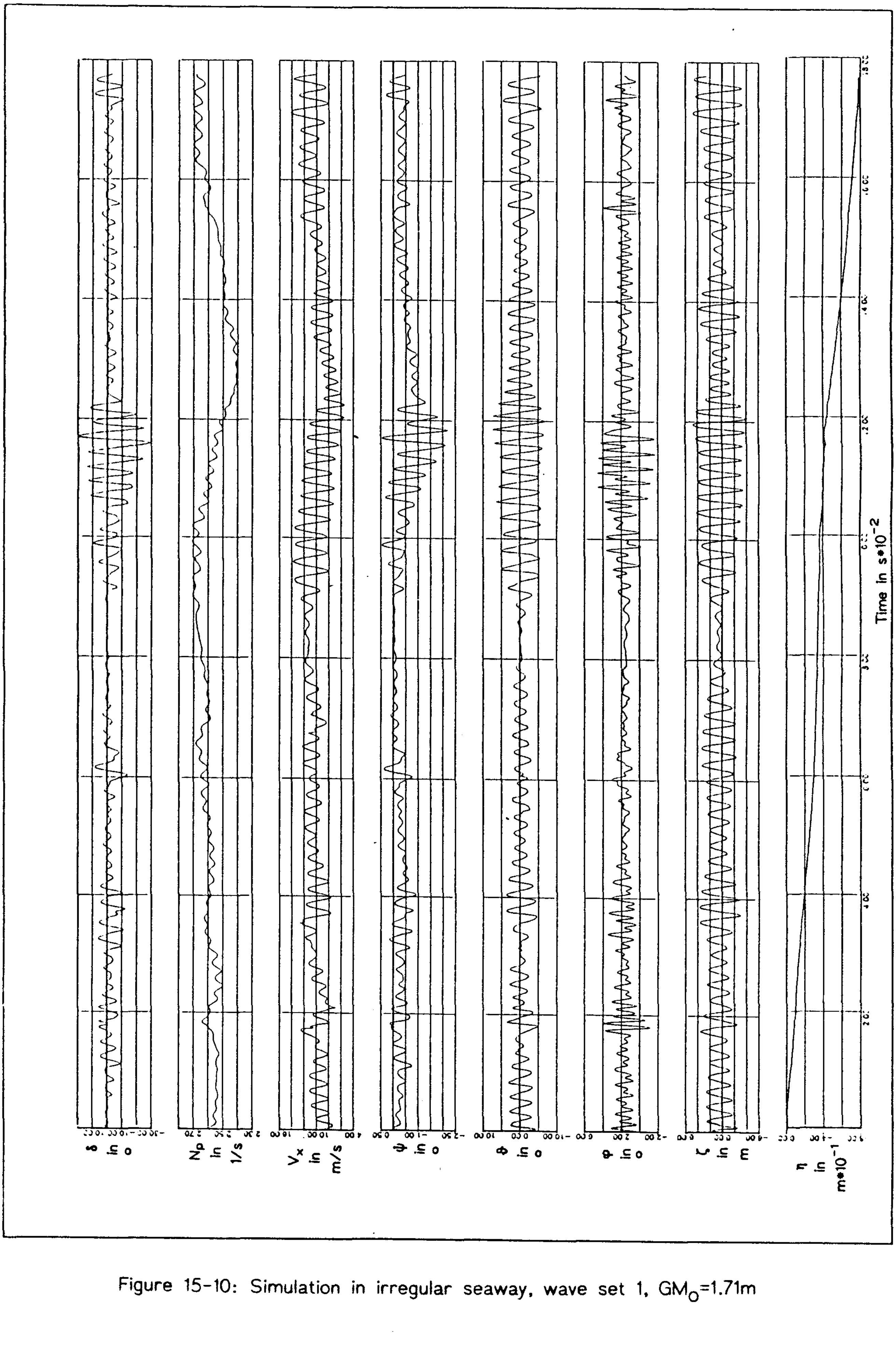

Figure 15-10: Simulation in irregular seaway, wave set 1, GM_O=1.71m

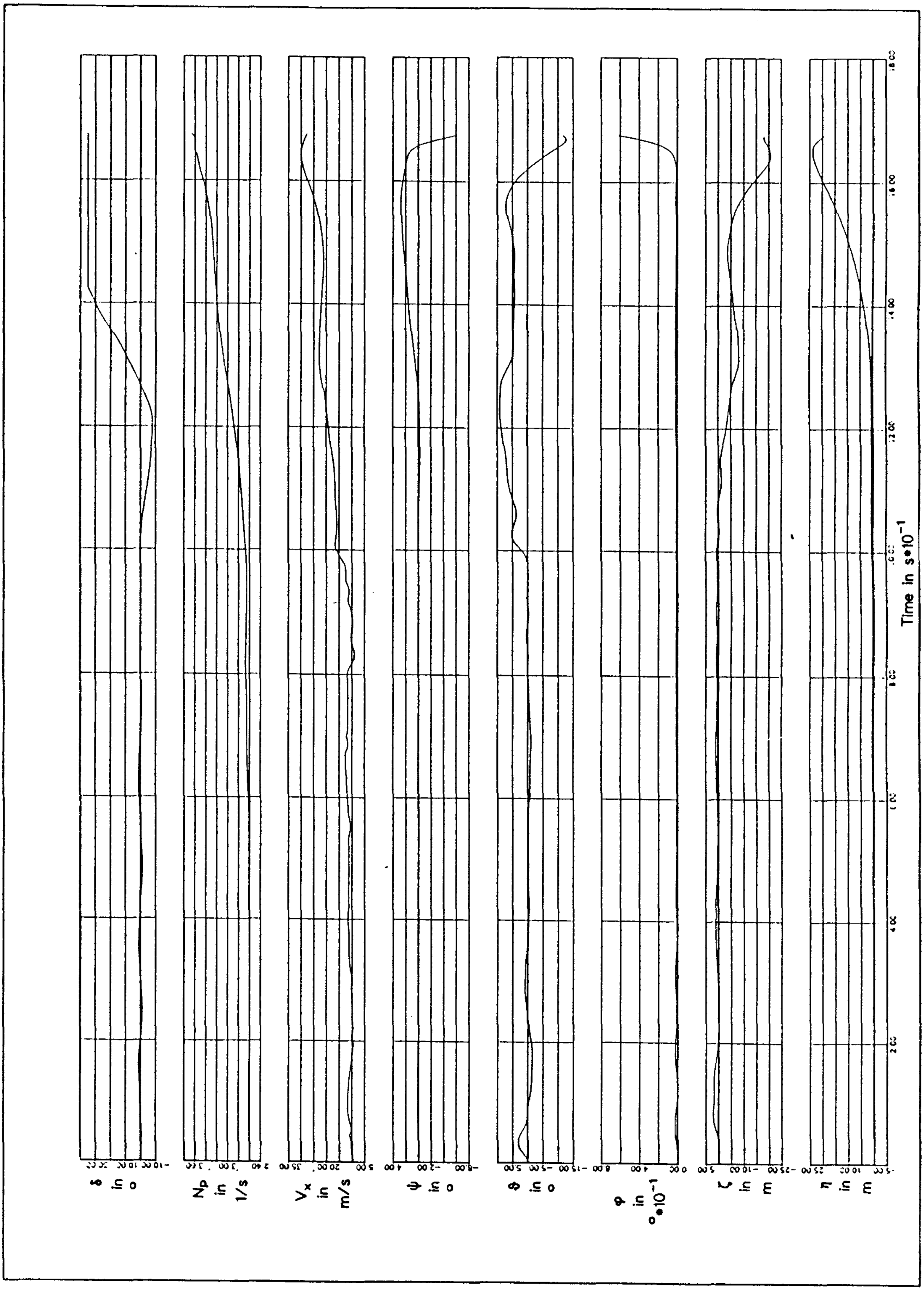

Figure 15-11: Simulation in irregular seaway, wave set 2, GM_O=1.71m

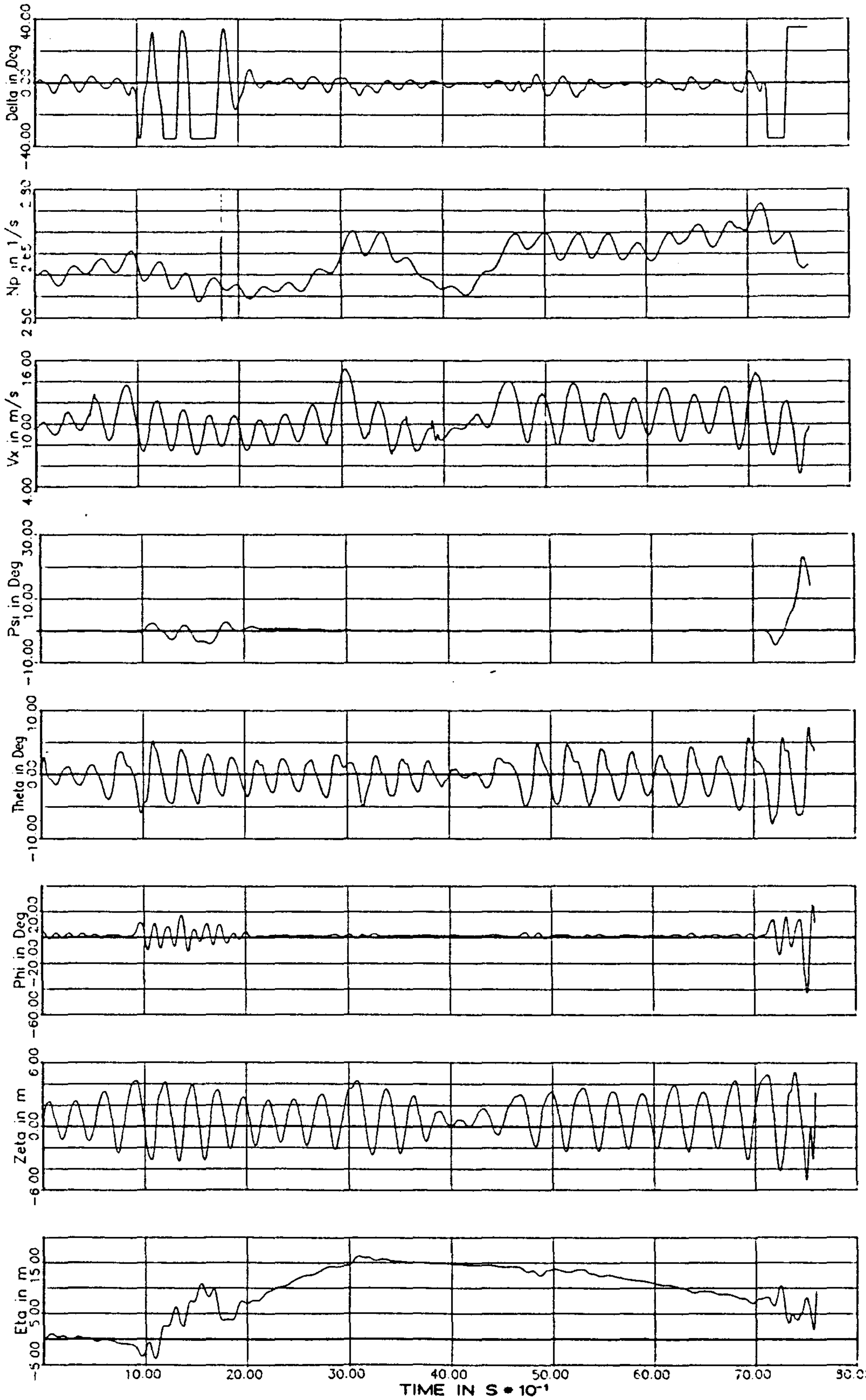

Figure 15-12: Simulation in irregular seaway, wave set 3, GM_O=1.71m

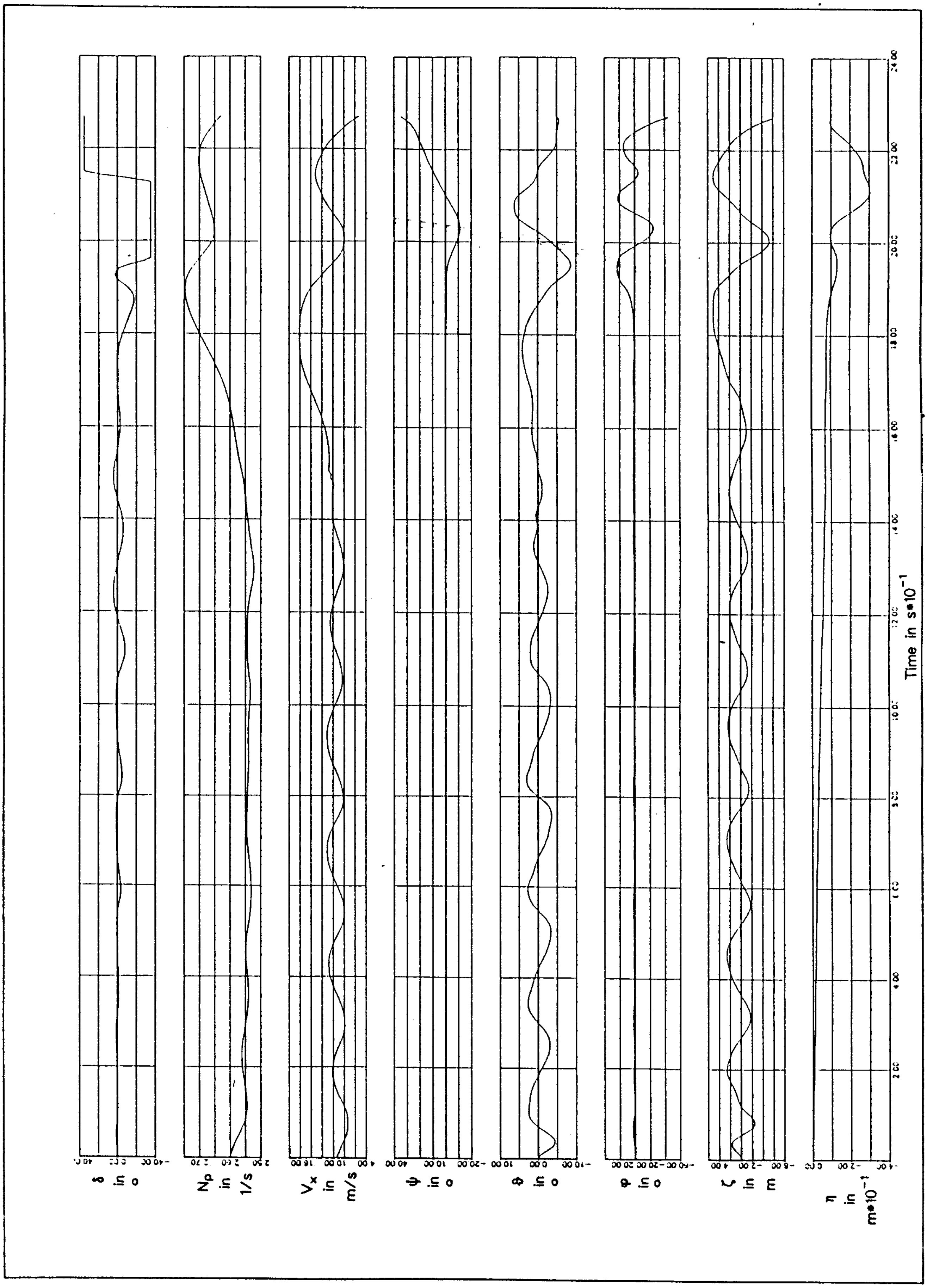

Figure 15-13: Simulation in irregular seaway, wave set 1, GM_O=1.85m

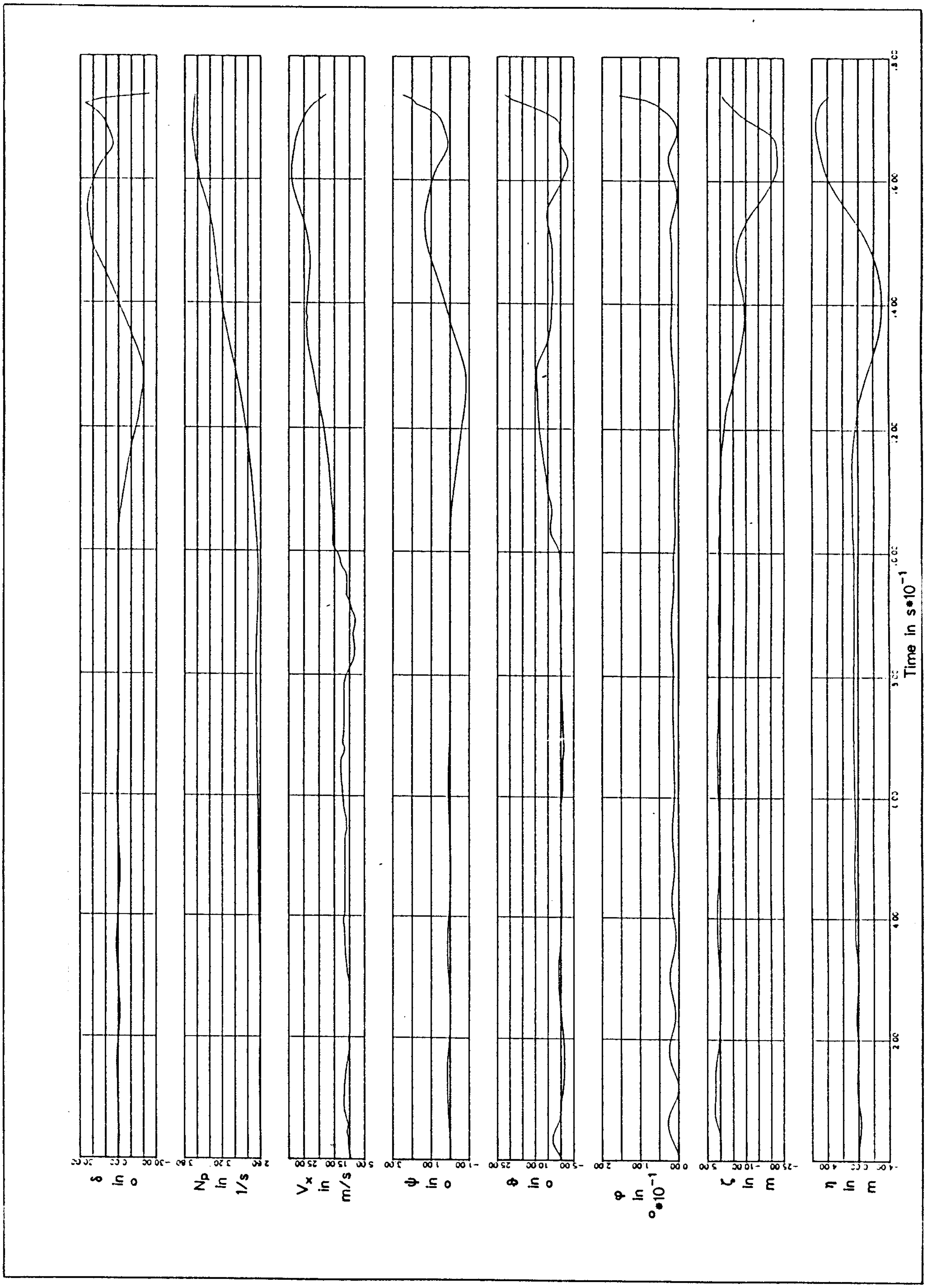

Figure 15-14: Simulation in irregular seaway, wave set 2, GM_0=1.85m

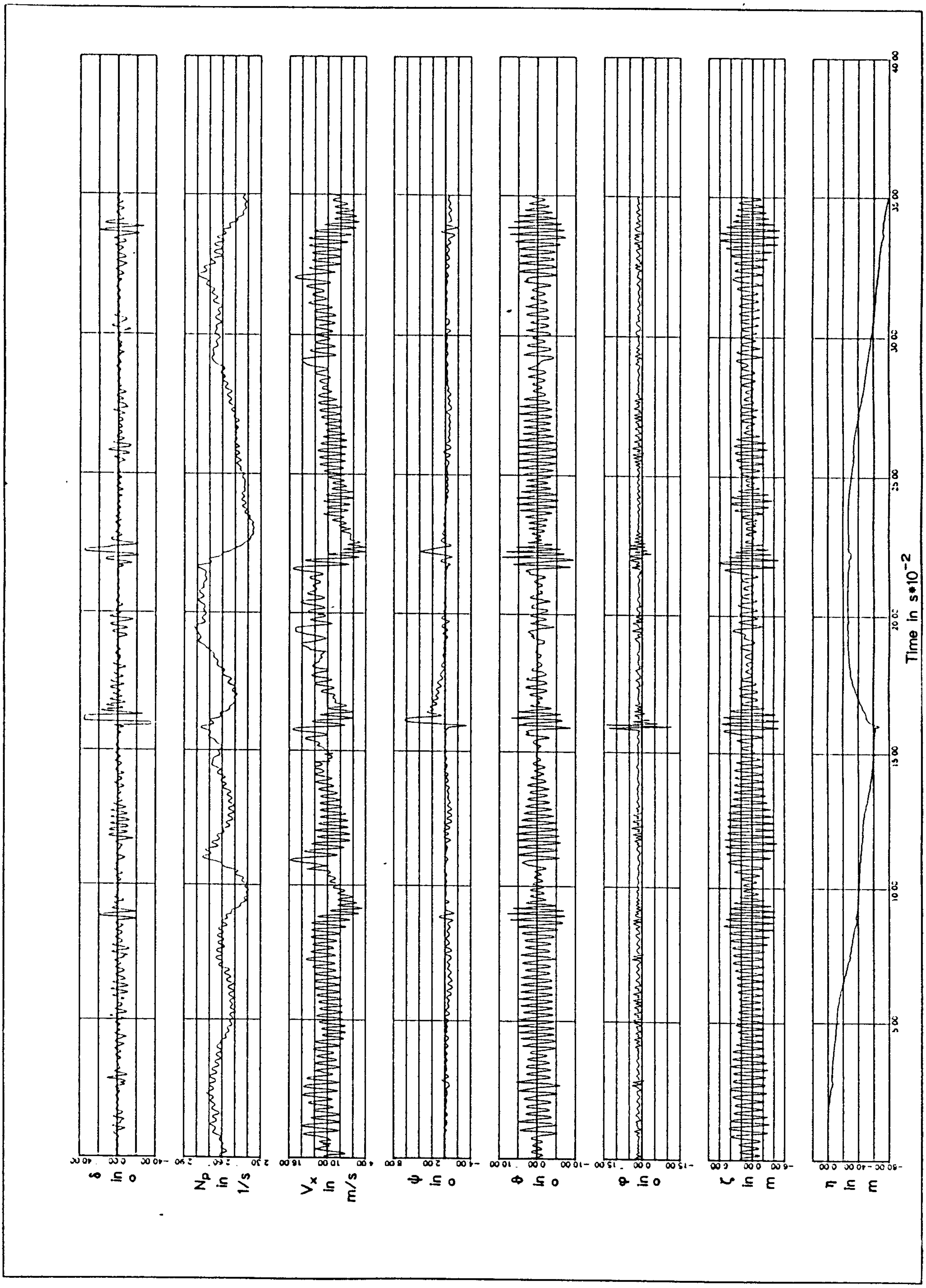

Figure 15-15: Simulation in irregular seaway, wave set 3, GM_O=1.85m

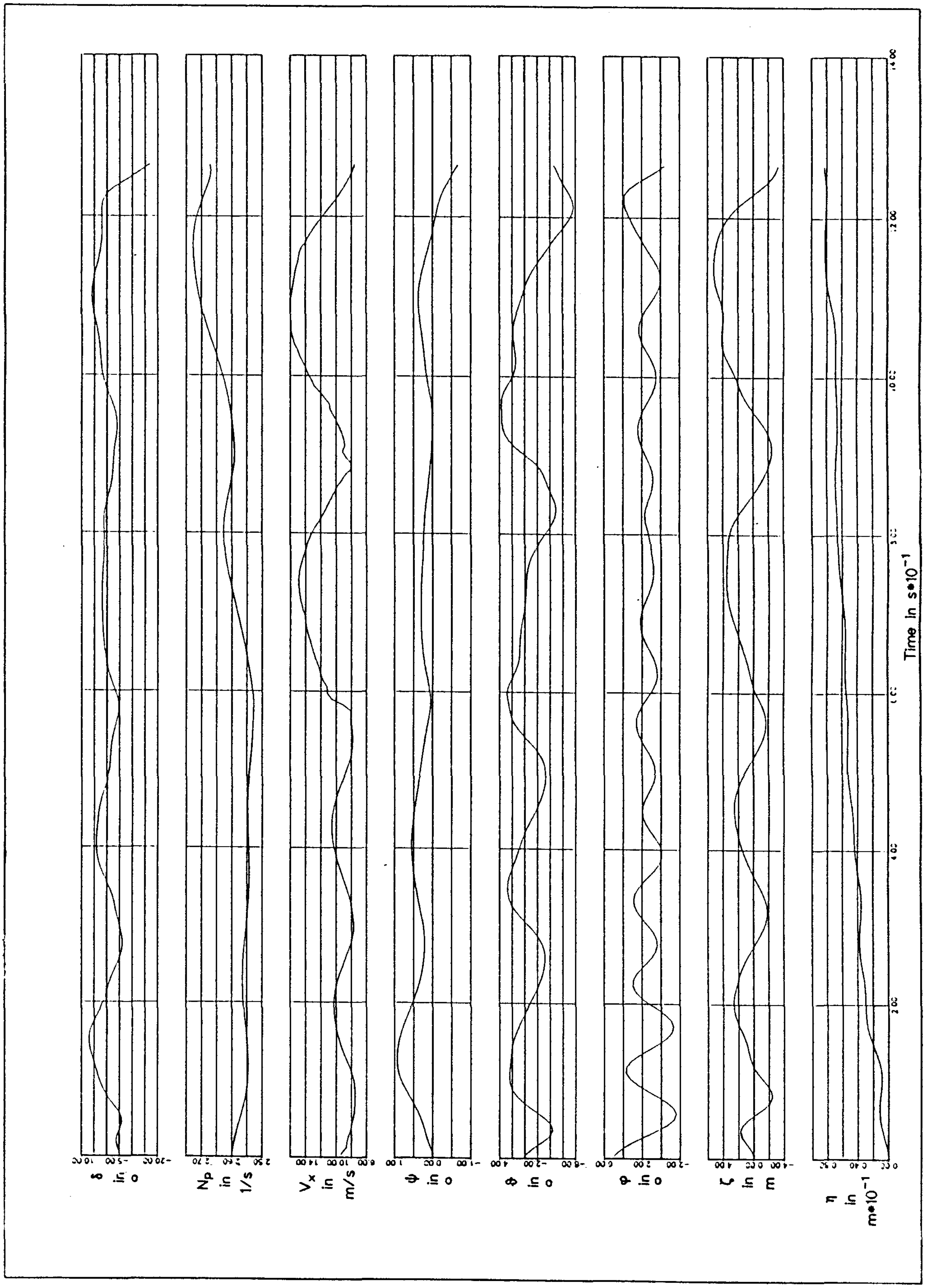

Figure 15-16: Simulation in irregular seaway, wave set 1, GM_0=2.14m

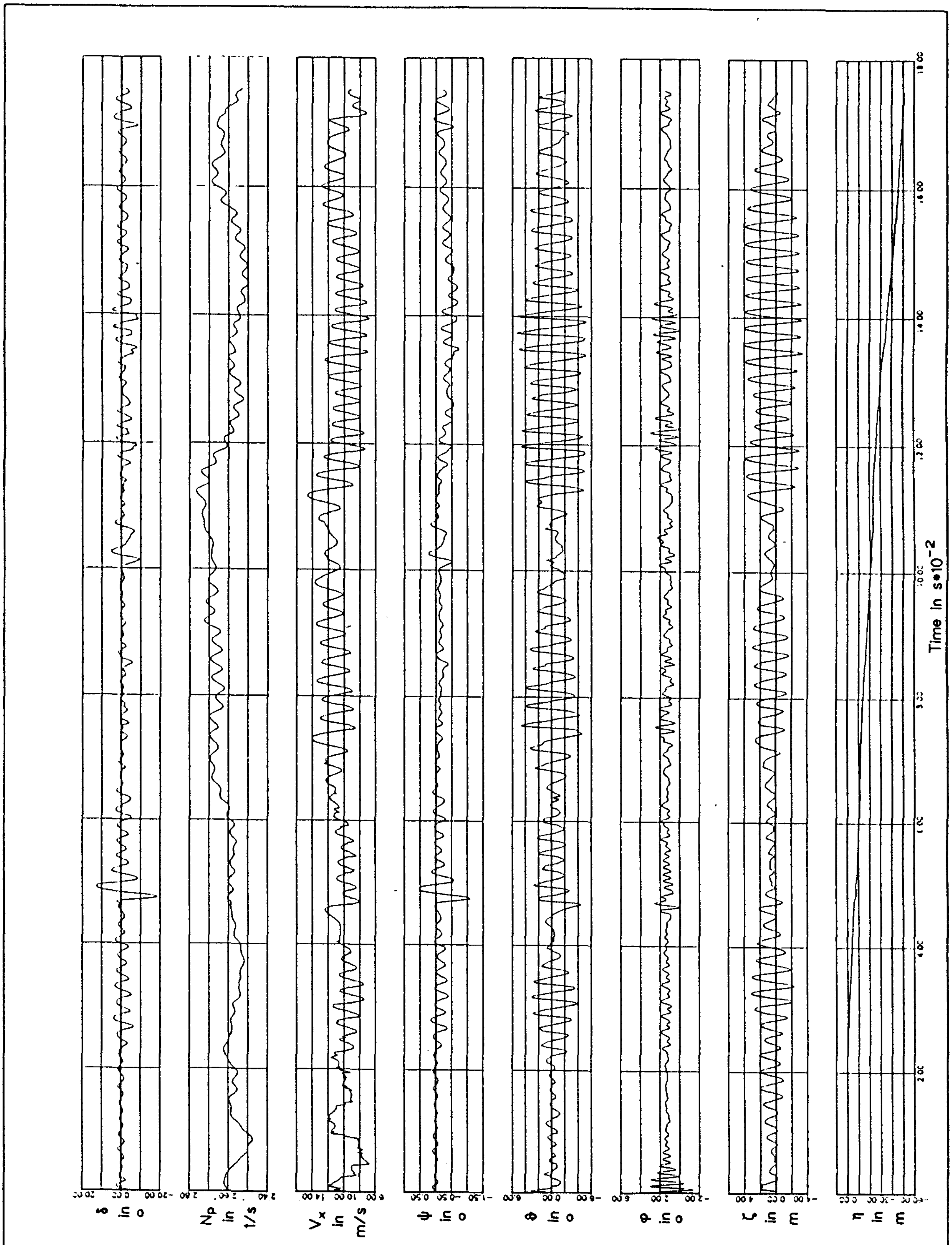

Figure 15-17: Simulation in irregular seaway, wave set 2, GM_o=2.14m

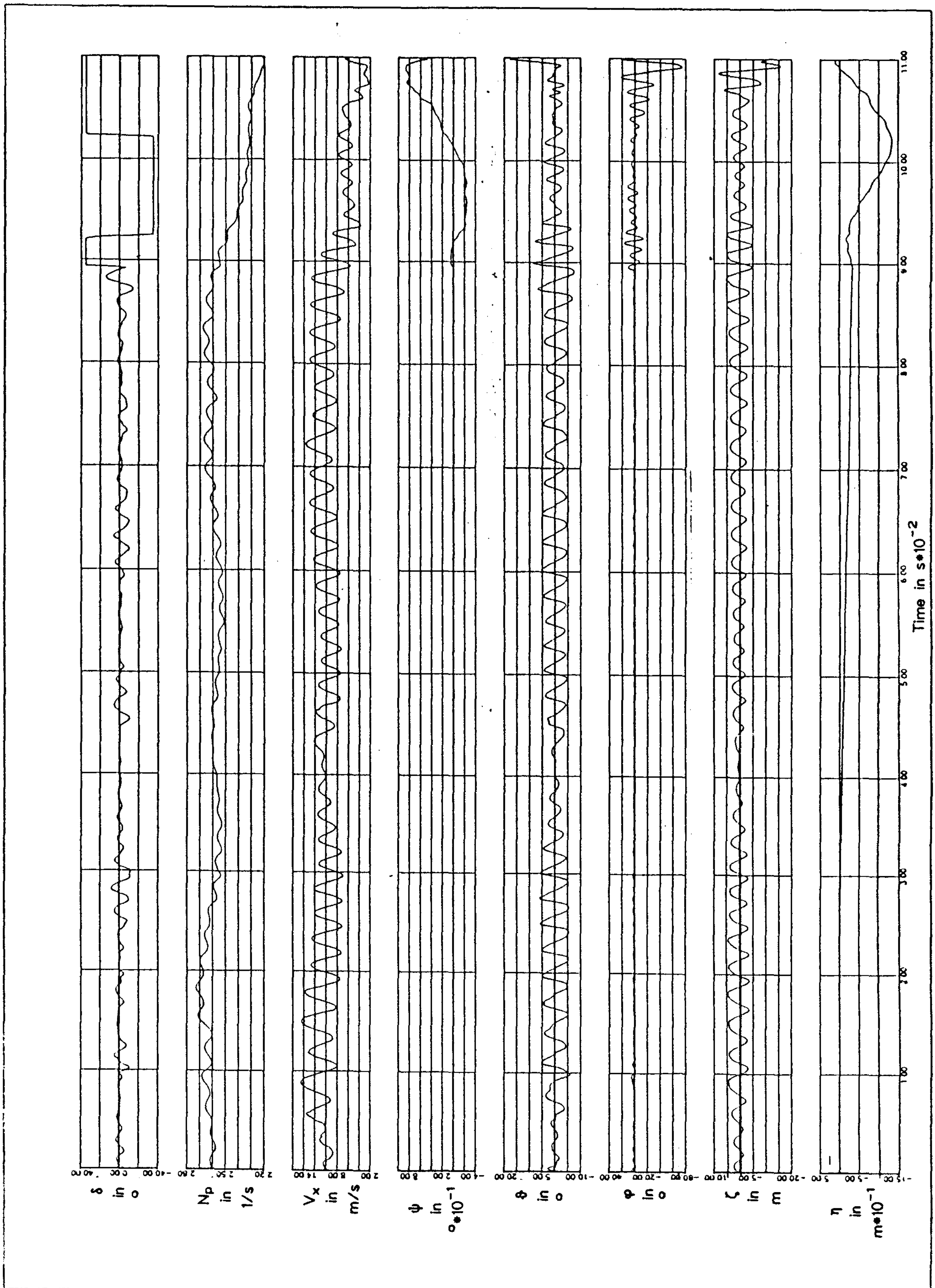

Figure 15-18: Simulation in irregular seaway, wave set 3, GM_o=2.14m

16 Conclusions

A method for the simulation of large amplitude ship motions in six degrees of freedom has been presented which includes all of the major forces acting on a ship. The comparison with model experiments in regular following waves shows a similar behaviour of the ship in the simulation. The maximum roll angles encountered in the simulation and the capsizing events agree fairly well with the experiments. As in the experiments, where a rudder of nearly the double the size of the original was used (tests in regular waves only), the inability of the ship to keep course presented a problem. The simulation of ship motions in following seas with low forward speeds could not be conducted under proper conditions, because the ship could not be held on course. This is a kind of behaviour which cannot possibly be treated with linear methods.

The comparison with model experiments in irregular following seas shows disagreement concerning the limiting value for the metacentric height at the border between safe and unsafe against capsizing. Although the general behaviour of the ship appears similar to that in the experiments, capsizes occured with metacentric heights well above the limiting value found in the experiments. Capsizes were almost every time linked with a large course deviation or even broaching to. Again this is a behaviour which cannot be simulated using linear methods.

There is still room for improvements of this simulation method. Some deficiencies in the calculation of the Froude-Krilov forces, which were allowed for on account of computational efficiency could be remedied by calculating these forces exactly from the pressure distribution on the ship's hull. The increase in the required computation time will in the future be offset by increases in the speed of computers anyway. Methods for establishing input data such as the drag coefficients of the ship sections for transverse flow are required. Further investigation is needed into the problem of steering in following seas and the selection of suitable constants for the auto-pilot. If simulations are being done for large wave amplitudes the ship should not be exposed to the full force of the waves right from the start. Instead the simulation should start with low wave heights, which should then be increased slowly. In this way it should be possible to eliminate problems due to errors in the initial values for the simulation variables.

The effort required for generating the necessary input data for the simulation program, particularly for calculating the hydrodynamic coefficient matrices A and B introduced in chapter 6, is very large. The computation time needed for the actual simulation is also very large. This method is therefore unsuitable for every day use in, for instance, a design office. It can be used, though, for systematic research into the behaviour of ships in extreme sea states, where the faster linear or partly linear methods (such as [16]) fail to give correct results.

The method can be easily extended to include additional forces and moments. It can also be extended without too much effort for establishing loads on the ship structure, such as the longitudinal bending moments and shear forces.

Appendix A: References

[1] W. Abicht, Die Sicherheit der Schiffe im nachlaufenden unregelmäßigen Seegang, Bericht Nr. 274, Institut für Schiffbau, Hamburg, 1971

[2] W. Blendermann, Windkräfte am Schiff, Bericht Nr. 467, Institut für Schiffbau, Hamburg, 1986

[3] P. Blume, Experimentelle Bestimmung von Koeffizienten der wirksamen Rolldämpfung und ihre Anwendung zur Abschätzung extremer Rollwinkel, Report No. 1511, Hamburgische Schiffbau-Versuchsanstalt (HSVA), March 1979

[4] P. Blume, H.-G. Hattendorff, An Investigation on Intact Stability of Fast Cargo Liners, Second International Conference on Stability of Ships and Ocean Vehicles, Tokyo, Oct. 1982

[5] P. Blume, H.G. Hattendorff, Stabilität und Kentersicherheit moderner Handelsschiffe, Bericht Nr. S 165/83, Hamburgische Schiffbau-Versuchsanstalt GmbH, 1983

[6] W. Froude, On the Rolling of Ships, Transactions INA, Vol. 2, 1861

[7] M. Fujino, B.S. Yoon, A Practical Method of Estimating Ship Motions and Wave Loads in Large Amplitude Waves, International Shipbuilding Progress, Vol. 33., No. 385, Sept. 1986

[8] O. Grim, Rollschwingungen, Stabilität und Sicherheit im Seegang, Schiffstechnik, 1952

[9] O. Grim, P. Schenzle, Die Berechnung der Torsionsbelastung eines Schiffes im Seegang, Bericht No. 236, Institut für Schiffbau, Hamburg, 1969

[10] S. Grochowalski, I. Rask, P. Söderberg, An Experimental Technique For Investigation Into the Physics of Ship Capsizing, Third International Conference on Stability of Ships and Ocean Vehicles, Gdansk, Sept. 1986

[11] H.G. Jacob, Rechnergestützte Optimierung statischer und dynamischer Systeme, Springer-Verlag, Berlin-Heidelberg-New York, 1982

[12] E.R. Jefferys, Simulation of wave power devices, Applied Ocean Research, 1984, Vol. 6, No. 1

[13] S. Kastner, Das Kentern von Schiffen in unregelmäßiger längslaufender See, Schiffstechnik, 1969/70

[14] B.V. Korvin-Kroukovsky, W.R. Jacobs, Pitching and Heaving Motion of a Ship in Regular Waves, Trans. SNAME, 1957

[15] A. Krilov, A General Theory of the Oscillations of a Ship on Waves, Transactions INA, 1898

[16] H.–P. Kröger, Rollsimulation von Schiffen im Seegang, Schiffstechnik Bd. 33, 1986

[17] J.B. Roberts, A Stochastic Theory for Nonlinear Ship Rolling in Irregular Seas, Journal of Ship Research, Vol. 26, No. 4, Dec. 1982, pp. 229-245

[18] J.B. Roberts, Effect of Parametric Excitation on Ship Rolling Motion in Random Waves, Journal of Ship Research, Vol. 26, No. 4, Dec. 1982, pp. 246-253

[19] N. Salvesen, E.O. Tuck, O. Faltinsen, Ship Motions and Sea Loads, Trans. SNAME, 1970

[20] M. Schmiechen, Zur Kollisionsdynamik von Schiffen, Jahrbuch der STG, 1974

[21] H. Söding, Schwimmfähigkeit und Stabilität, Bericht Nr. 11 des Instituts für Entwerfen von Schiffen und Schiffstheorie, Universität Hannover, 1975

[22] H. Söding, Eine Modifikation der Streifenmethode, Schiffstechnik No. 80, 1969

[23] H. Söding, Leckstabilität im Seegang, Bericht Nr. 429 des Instituts für Schiffbau der Universität Hamburg, Dec. 1982

[24] H. Söding, Prediction of Ship Steering Capabilities, Schiffstechnik Bd. 29, 1982

[25] B. Wagner, Windkräfte an Überwasserschiffen, Jahrbuch der STG, 1967

Appendix B: Approximation of the Waterline

The waterline at a section is approximated by a straight line using the method described in [23].
A harmonic function of the form

$$f(x) = f_1 \cdot \cos(k \cdot x) + f_2 \cdot \sin(k \cdot x) \tag{B.1}$$

is approximated by a straight line in the interval $|x| \leq x_1$ according to the method of least squares. If the equation of the straight line is given by $y = a + bx$, then the following integral must be minimised:

$$\int_{-x_1}^{x_1} (f(x) - y)^2 \, dx$$

This integral has a minimum, if the constants a and b are chosen in the following way:

$$a = f(0) \cdot \frac{\sin(k \cdot x_1)}{k \cdot x_1} \tag{B.2}$$

$$b = \frac{df}{dx}(x{=}0) \cdot \frac{3}{(k \cdot x_1)^3} \cdot \left(\sin(k \cdot x_1) - k \cdot x_1 \cdot \cos(k \cdot x_1)\right) \tag{B.3}$$

For approximating the waterline in a section plane the component of the wave number in the section plane, which is given by

$$k_{j1} = k_j \cdot \sin(\mu_j + \psi), \tag{B.4}$$

is used for calculating the correction factors r_{j1} and r_{j2}.

$$r_{j1} = \frac{\sin(k_{j1} \cdot x_1)}{k_{j1} \cdot x_1} \tag{B.5}$$

$$r_{j2} = \frac{3}{(k_{j1} \cdot x_1)^3} \cdot \left(\sin(k_{j1} \cdot x_1) - k_{j1} \cdot x_1 \cdot \cos(k_{j1} \cdot x_1)\right) \tag{B.6}$$

r_{j1} is used for calculating the wave height at the midpoint of the section waterline according to (5.3). r_{j2} is used for calculating the inclination of the water surface in ξ- and η-direction according to (5.4) and (5.5) at the midpoint of the section waterline.

Appendix C: Calculating Matrices A and B

For calculating the radiation and diffraction forces a method is required for determining the matrices A and B introduced in chapter 6.
Matrices A and B are the coefficients of a ratio-of-polynomials used to approximate added mass and damping in the frequency domain:

$$\left[\sum_{k=0}^{kk} B_k \cdot (i\omega)^k\right]^{-1} \cdot \sum_{k=0}^{kk} A_k \cdot (i\omega)^k \approx -M(\omega) + \frac{i}{\omega} \cdot N(\omega) \tag{C.1}$$

A number of discrete frequencies is used for calculating A and B. The added mass and damping matrices are normalized using a normalization matrix T_N:

$$T_N = \begin{bmatrix} t_{n1} & 0 & 0 \\ 0 & t_{n2} & 0 \\ 0 & 0 & t_{n3} \end{bmatrix} \tag{C.2}$$

with

$$t_{ni} = \frac{1}{\frac{1}{n_\omega} \cdot \sum_{n=1}^{n_\omega} \sqrt{m_{iin}^2 + \left(\frac{n_{iin}}{\omega_n}\right)^2}} \tag{C.3}$$

n_ω is the number of frequencies. m_{iin} and n_{iin} are components of the added mass and damping matrix for frequency n respectively.
(C.1) is thus transformed to:

$$T_N \cdot \left[\sum_{k=0}^{kk} B_k \cdot (i\omega_n)^k\right]^{-1} \cdot \sum_{k=0}^{kk} A_k \cdot (i\omega_n)^k \cdot T_N \approx T_N \cdot \left(-M(\omega_n) + \frac{i}{\omega} \cdot N(\omega_n)\right) \cdot T_N \tag{C.4}$$

Since T_N is a diagonal matrix this equation can also be written as:

$$\left[\sum_{k=0}^{kk} B_k \cdot (i\omega_n)^k\right]^{-1} \cdot \sum_{k=0}^{kk} T_N \cdot A_k \cdot T_N \cdot (i\omega_n)^k \approx T_N \cdot \left(-M(\omega_n) + \frac{i}{\omega} \cdot N \omega_n)\right) \cdot T_N \tag{C.5}$$

Transformed matrices A_{Nk} can be introduced, defined as $A_{Nk} = T_N \cdot A_k \cdot T_N$. The difference between both sides of the equation is then given by the matrix D:

$$D_n = \left[\sum_{k=0}^{kk} B_k \cdot (i\omega_n)^k\right]^{-1} \cdot \sum_{k=0}^{kk} A_{Nk} \cdot (i\omega_n)^k - T_N \cdot \left(-M(\omega_n) + \frac{i}{\omega} \cdot N(\omega_n)\right) \cdot T_N \tag{C.6}$$

To obtain the best approximation of added mass and damping the sum of the squares of all elements of this difference matrix for all frequencies has to be minimised:

$$\sum_n \sum_i \sum_j |D_{ijn}|^2 \stackrel{!}{=} \text{min.} \tag{C.7}$$

Here n is an index for the frequency, i and j are indices for the matrix elements.

The minimisation is performed using an optimisation procedure published in [11] (Fortran subroutine EXTREM).

The results of the minimisation are the matrices A_{Nk} and B_k. The matrices A_k are obtained from the A_{Nk} by the inverse of the normalization:

$$A_k = T_N^{-1} \cdot A_{Nk} \cdot T_N^{-1} \tag{C.8}$$

The number of unknowns in the optimisation can be reduced, if the boundary conditions for infinite frequency are observed. For infinite frequency the damping is zero, and the added mass asymptotically approaches a value we shall term M_∞. From (C.1) the following equations can be derived for infinite frequency:

$$B_{kk}^{-1} \cdot A_{kk} = -M_\infty \tag{C.9}$$

$$B_{kk-1}^{-1} \cdot A_{kk-1} = -M_\infty \tag{C.10}$$

As stated in chapter 6 B_{kk} is set equal to the unit matrix, which leads to:

$$A_{kk} = -M_\infty \tag{C.11}$$

A_{kk-1} can be calculated from (C.10), if B_{kk-1} is known. Therefore only A_O to A_{kk-2} and B_O to B_{kk-1} need be calculated in the optimisation program. A further reduction of the number of unknowns is achieved by reducing the B-matrices to diagonal matrices. The results prove that nontheless a very good approximation of the added mass and damping can be achieved with kk as low as 2.
An example of such an approximation using kk = 2 is shown in figure C-1. The added mass and damping matrix elements are plotted as a function of the circular frequency ω. The drawn out lines represent the values calculated from potential theory. The asterisks mark the values obtained from the left hand side of (C.1).

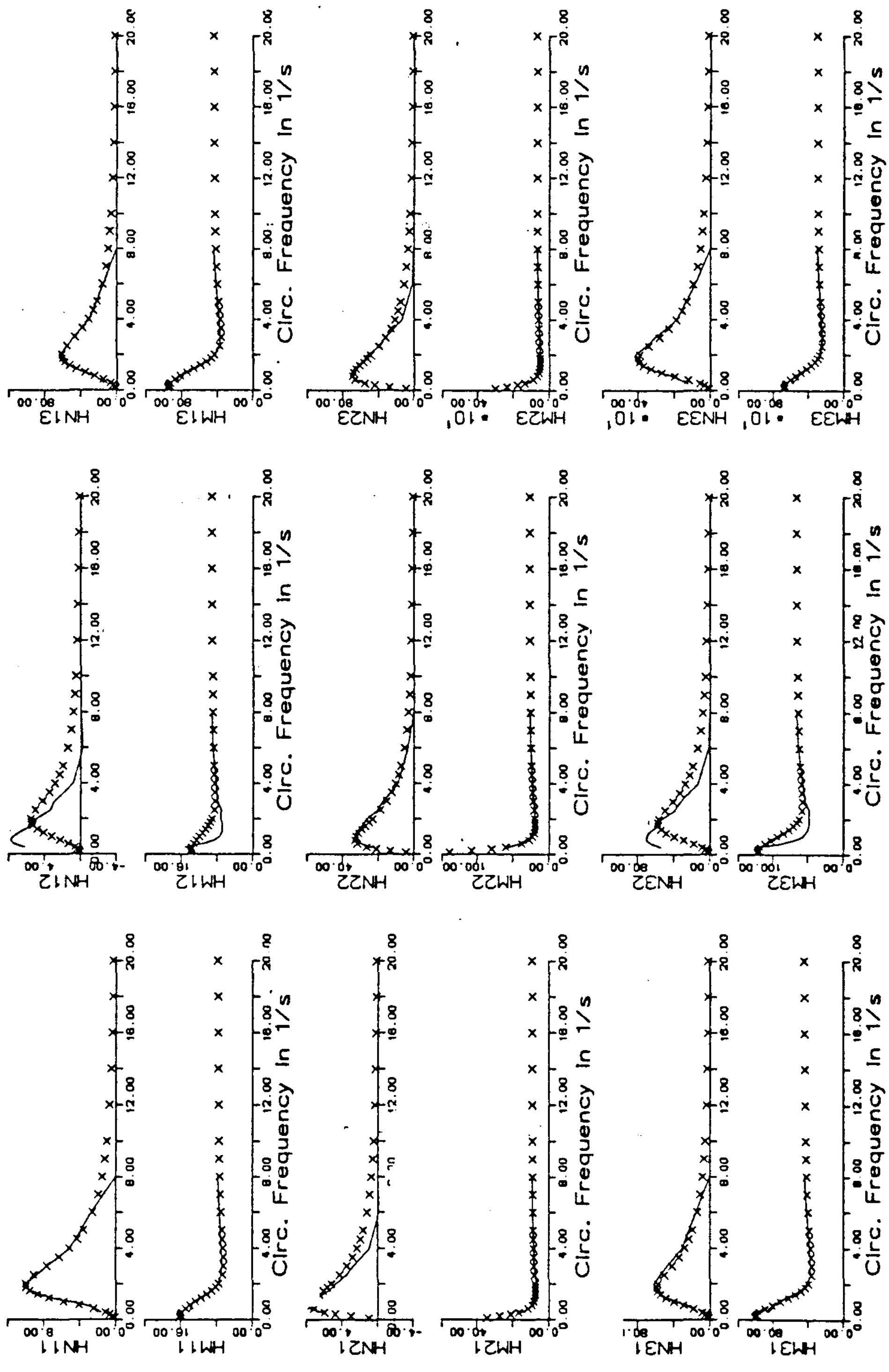

Figure C-1: Comparison between added mass and damping fr ship section calculated by potential theory (drawn out lines) and approximated using A and B coefficients (Xs), for kk = 2, HM is the added mass, HN is the damping, the numbers represent the indexes of the matrix elements

Appendix D: Orbital Velocity and Acceleration

The velocity potential Φ of the seaway at the point (ξ,η,ζ) is given by:

$$\Phi = \sum_j \frac{\omega_j}{k_j}\cdot\zeta_j\cdot e^{-k_j\cdot(\zeta+d)}\cdot\sin(\omega_j\cdot t - k_j\cdot\xi\cdot\cos\mu_j + k_j\cdot\eta\cdot\sin\mu_j) \tag{D.1}$$

Let us introduce the following abbreviations:

$$a_j = \omega_j\cdot t - k_j\cdot\xi\cdot\cos\mu_j + k_j\cdot\eta\cdot\sin\mu_j \tag{D.2}$$

$$b_j = \omega_j\cdot r_{j1}\cdot\zeta_j\cdot e^{-k_j\cdot(\zeta+d)} \tag{D.3}$$

For the calculation of the orbital velocities the correction factor r_{j1} for the waterline, which is used in the calculation of the Froude-Krilov forces (appendix B), is also used.
The orbital velocities are the derivatives of the velocity potential Φ in the respective directions:

$$\frac{\partial\Phi}{\partial\xi} = \dot{u}_{Orb\xi} = -\sum_j b_j\cdot\cos\mu_j\cdot\cos a_j \tag{D.4}$$

$$\frac{\partial\Phi}{\partial\eta} = \dot{u}_{Orb\eta} = \sum_j b_j\cdot\sin\mu_j\cdot\cos a_j \tag{D.5}$$

$$\frac{\partial\Phi}{\partial\zeta} = \dot{u}_{Orb\zeta} = -\sum_j b_j\cdot\sin a_j \tag{D.6}$$

The orbital accelerations are the time derivatives of the orbital velocities:

$$\ddot{u}_{Orb\xi} = \sum_j \omega_j\cdot b_j\cdot\cos\mu_j\cdot\sin a_j \tag{D.7}$$

$$\ddot{u}_{Orb\eta} = -\sum_j \omega_j\cdot b_j\cdot\sin\mu_j\cdot\sin a_j \tag{D.8}$$

$$\ddot{u}_{Orb\zeta} = -\sum_j \omega_j\cdot b_j\cdot\cos a_j \tag{D.9}$$

These velocities and accelerations are given in the earth coordinate system. If they are required in the ship coordinate system, they can be transformed according to the following formulae:

$$\underline{\dot{u}}_{Orbx} = T^{-1}\cdot\underline{\dot{u}}_{Orb\xi} \tag{D.10}$$

$$\underline{\ddot{u}}_{Orbx} = T^{-1}\cdot\underline{\ddot{u}}_{Orb\xi} \tag{D.11}$$

Angular orbital velocity and acceleration

An effective angular orbital velocity for a ship's section is calculated approximately from the orbital velocities at 4 points as indicated in the following drawing.
The draught d is a mean draught, given by section area divided by mean section

breadth b. The angular orbital velocity follows from applying the torque exerted by each velocity vector:

$$\dot{u}_{Orb\omega} = \frac{\dot{u}_{oz1} - \dot{u}_{oz2} + \dot{u}_{oy1} - \dot{u}_{oy2}}{b + d} \tag{D.12}$$

The angular orbital acceleration is calculated similarly, substituting velocities by accelerations.

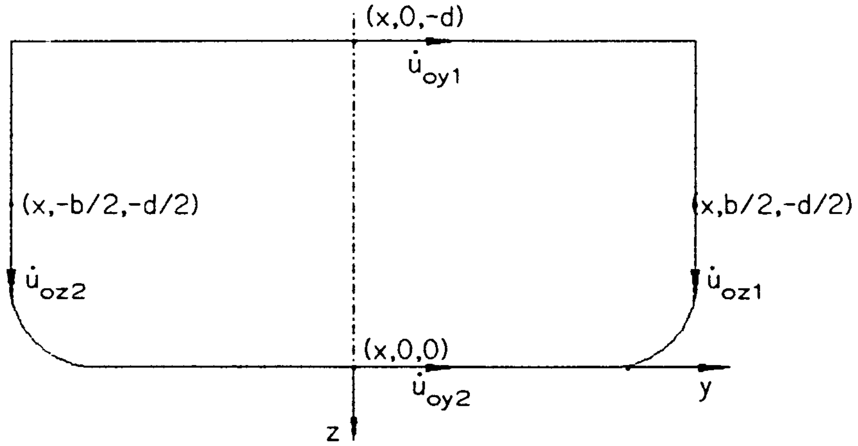

Appendix E: Ship A

Main Particulars

Length b.p.	135.0 m
Breadth	23.0 m
Depth	10.7 m
Draught	8.2 m
Displacement	17190 m^3

Simulation Data

Moments of inertia

$$I_G = \begin{bmatrix} 1098000 & 0 & 0 \\ 0 & 19800000 & 0 \\ 0 & 0 & 20250000 \end{bmatrix} tm^2$$

Ship's mass: m = 17275 t

Longitudinal centre of gravity: -1.22m forward of amidships

Number of sections for hydrostatic and hydrodynamic data: 11

Draughts for hydrostatic data: from -3.0m to 13.0m in steps of 1.0m
Inclination angles for hydrostatic data: from 0° to 90° in steps of 5°

Draughts for A- and B-matrices: from -5.0m to 17.0m in steps of 2.0m
Inclination angles for A- and B-matrices: from 0° to 90° in steps of 10°

Resistance data: CR = 2.0, Exponent = 2.5

Roll damping coefficients

Fn	B_L in kNms	B_Q in $kNms^2$
0.0	7889	191150
0.1	11833	293843
0.2	29364	227568

Drag coefficients for transverse resistance: 1.0 for all sections

Propeller and Propulsion Data

Number of propellers:	1
Propeller diameter:	5.6m
blade area ratio:	0.7
Pitch:	4.9m
Number of blades:	4
Thrust deduction fraction:	0.192
Wake fraction:	0.287
Mechanical efficiency:	0.99
Moment of inertia of prop.:	$10000 tm^2$
Propeller position	(-64.7, 0.0, 3.2) m

Rudder Data

Trailing edge at	-58.7m
Lift centre at	-67.5m
Chord length	3.85m
r	1.0
c_{DR}	1.0

Immersion 1.1m

Rudder area: $1.89m^2$ a_H: 0.0001624

Δx_L: 0.0863 Λ: 0.62

v_a: 0.3	c_{L1}: 0.3142	v_a/v_m: 0.9991
v_a: 2.1	c_{L1}: 0.3142	v_a/v_m: 0.9991
v_a: 3.9	c_{L1}: 0.3142	v_a/v_m 0.9991
v_a: 5.7	c_{L1}: 0.1077	v_a/v_m: 0.2736
v_a: 7.5	c_{L1}: 0.1635	v_a/v_m: 0.4022
v_a: 9.3	c_{L1}: 0.2329	v_a/v_m: 0.6252

Immersion 2.6m

Rudder area: $6.83m^2$ a_H: 0.0009095

Δx_L: 0.4283 Λ: 2.15

v_a: 0.30	c_{L1}: 0.4945	v_a/v_m: 0.0300
v_a: 2.1	c_{L1}: 0.5585	v_a/v_m: 0.1610
v_a: 3.9	c_{L1}: 0.6205	v_a/v_m: 0.2858
v_a: 5.7	c_{L1}: 0.6833	v_a/v_m: 0.4186
v_a: 7.5	c_{L1}: 0.7600	v_a/v_m: 0.5822
v_a: 9.3	c_{L1}: 0.8719	v_a/v_m: 0.7902

Immersion 4.1m

Rudder area: $11.8m^2$ a_H: 0.002176

Δx_L: 0.9212 Λ: 3.65

v_a:	0.30	c_{L1}:	1.0427	v_a/v_m:	0.0355
v_a:	2.1	c_{L1}:	1.1077	v_a/v_m:	0.1872
v_a:	3.9	c_{L1}:	1.1592	v_a/v_m:	0.3278
v_a:	5.7	c_{L1}:	1.2102	v_a/v_m:	0.4770
v_a:	7.5	c_{L1}:	1.3249	v_a/v_m:	0.6506
v_a:	9.3	c_{L1}:	1.4381	v_a/v_m:	0.8399

Immersion 5.6m

Rudder area: $16.1m^2$ a_H: 0.004015

Δx_L: 1.5118 Λ: 5.14

v_a:	0.30	c_{L1}:	2.1520	v_a/v_m:	0.0536
v_a:	2.1	c_{L1}:	2.1993	v_a/v_m:	0.2800
v_a:	3.9	c_{L1}:	2.1944	v_a/v_m:	0.4691
v_a:	5.7	c_{L1}:	2.1470	v_a/v_m:	0.6387
v_a:	7.5	c_{L1}:	2.1034	v_a/v_m:	0.7896
v_a:	9.3	c_{L1}:	1.9570	v_a/v_m:	0.8602

Immersion 7.1m

Rudder area: $21.0m^2$ a_H: 0.006187

Δx_L: 2.1709 Λ: 6.62

v_a:	0.30	c_{L1}:	2.3702	v_a/v_m:	0.0617
v_a:	2.1	c_{L1}:	2.5337	v_a/v_m:	0.3165
v_a:	3.9	c_{L1}:	2.5857	v_a/v_m:	0.5187
v_a:	5.7	c_{L1}:	2.5626	v_a/v_m:	0.6878
v_a:	7.5	c_{L1}:	2.5155	v_a/v_m:	0.8263
v_a:	9.3	c_{L1}:	2.4630	v_a/v_m:	0.9350

Appendix F: Wave Data for the Irregular Seaway

From the spectrum for the irregular seaway 1 as given in [4] wave components were derived. The frequency range from 0.28 to 1.03 s^{-1} was subdivided into as many strips of equal width as wave components were required. The frequency of each wave component was chosen randomly from within the range of the respective strip. The wave amplitude was calculated from the value of the spectrum at the middle of the strip. The phase angle was chosen randomly between 0° and 360°.
Using this procedure three sets of wave components were created, differing in the phase angles and slightly in the frequencies of the components. These wave sets 1 to 3 represent almost identical spectra, but lead to different time functions of the wave height.

Wave set 1, 41 components:

amplitude in m	c.freq. in 1/s	dir. in °	phase in °
0.1628	0.2825	0.0000	139.1993
0.2940	0.2950	0.0000	139.2833
0.3634	0.3160	0.0000	277.7288
0.4376	0.3369	0.0000	1.5268
0.5498	0.3579	0.0000	105.0516
0.6556	0.3630	0.0000	167.6532
0.8729	0.3832	0.0000	163.9607
1.4218	0.4159	0.0000	303.6905
1.6748	0.4207	0.0000	29.7418
1.8117	0.4521	0.0000	327.5439
1.9421	0.4628	0.0000	182.4863
1.9393	0.4858	0.0000	253.3185
1.7771	0.5026	0.0000	75.1445
1.5338	0.5254	0.0000	53.5735
1.2925	0.5340	0.0000	109.1977
1.1055	0.5497	0.0000	6.3801
0.9344	0.5641	0.0000	19.8214
0.7772	0.5963	0.0000	104.0591
0.6438	0.6099	0.0000	122.4161
0.5832	0.6332	0.0000	250.4734
0.5573	0.6488	0.0000	262.3804
0.5072	0.6612	0.0000	3.7504
0.4469	0.6845	0.0000	220.0011
0.3894	0.7080	0.0000	131.3089
0.3464	0.7251	0.0000	192.3354
0.3193	0.7327	0.0000	234.0651
0.2999	0.7529	0.0000	243.9604
0.2870	0.7694	0.0000	286.6945
0.27844	0.7834	0.0000	48.4652
0.2718	0.8064	0.0000	170.8224
0.2641	0.8295	0.0000	152.5591
0.2526	0.8488	0.0000	188.0197
0.2400	0.8580	0.0000	144.6733

amplitude in m	c.freq. in 1/s	dir. in °	phase in °
0.2278	0.8912	0.0000	49.4779
0.2161	0.9109	0.0000	179.9288
0.2048	0.9249	0.0000	229.2396
0.1941	0.9395	0.0000	343.3470
0.1838	0.9565	0.0000	117.8578
0.1750	0.9733	0.0000	163.1773
0.1706	0.9880	0.0000	283.3600
0.1721	1.0129	0.0000	136.2169

Spectrum of this seaway (S = energy density):

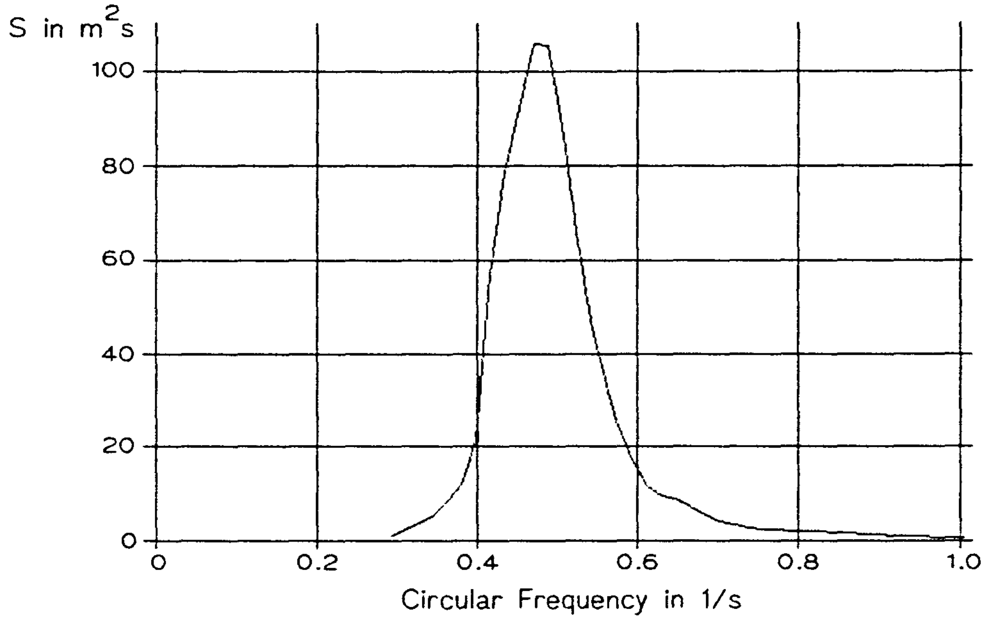

Wave height at the position (0,0) in m:

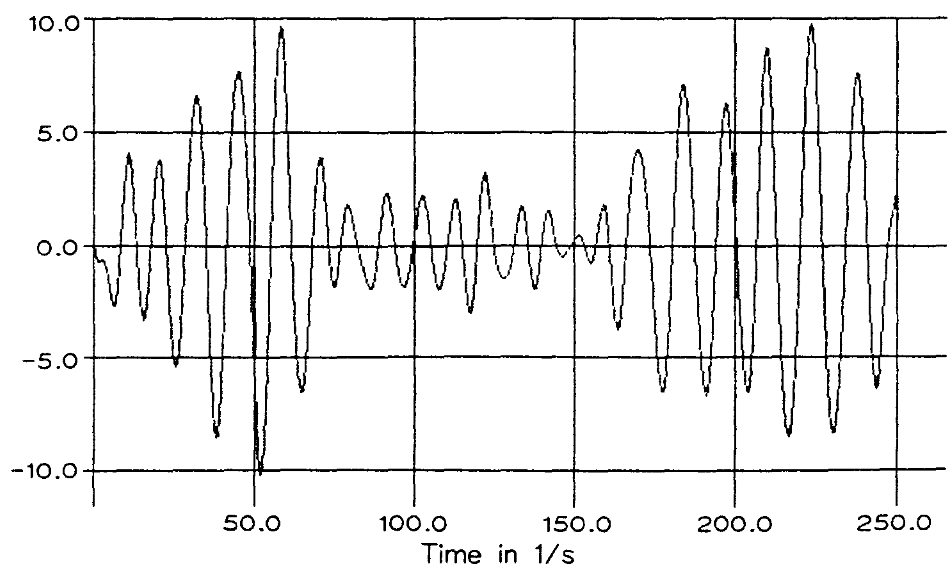

Wave set 2, 40 components:

amplitude in m	c.freq. in 1/s	dir. in °	phase in °
0.1671	0.2785	0.0000	164.8327
0.3010	0.2956	0.0000	134.4273
0.3719	0.3086	0.0000	348.2379
0.4514	0.3407	0.0000	201.6348
0.5685	0.3473	0.0000	82.9857
0.6844	0.3805	0.0000	195.2616
0.9382	0.3874	0.0000	124.0261
1.5140	0.4015	0.0000	200.4755
1.7286	0.4353	0.0000	295.1887
1.8690	0.4552	0.0000	257.4261
1.9849	0.4660	0.0000	53.6826
1.9282	0.4849	0.0000	45.2567
1.7279	0.4974	0.0000	245.3378
1.4645	0.5302	0.0000	339.0447
1.2380	0.5381	0.0000	82.4645
1.0503	0.5651	0.0000	226.5475
0.8788	0.5757	0.0000	206.2036
0.7205	0.5912	0.0000	181.6276
0.6153	0.6112	0.0000	285.2457
0.5773	0.6267	0.0000	121.2328
0.5419	0.6527	0.0000	32.7907
0.4809	0.6769	0.0000	202.8057
0.4187	0.6856	0.0000	193.6261
0.3658	0.7134	0.0000	148.9981
0.3329	0.7277	0.0000	323.1967
0.3099	0.7566	0.0000	356.5648
0.2943	0.7702	0.0000	170.5412
0.2843	0.7773	0.0000	36.3131
0.2771	0.7996	0.0000	226.9720
0.2697	0.8241	0.0000	140.9801
0.2588	0.8403	0.0000	152.3712
0.2457	0.8563	0.0000	27.9169
0.2330	0.8850	0.0000	180.9792
0.2207	0.9050	0.0000	113.4506
0.2089	0.9257	0.0000	78.5506
0.1977	0.9400	0.0000	5.8020
0.1870	0.9603	0.0000	212.7520
0.1776	0.9787	0.0000	233.4331
0.1728	0.9916	0.0000	208.6772
0.1742	1.0135	0.0000	115.6985

Wave set 3, 40 components:

amplitude in m	c.freq. in 1/s	dir. in °	phase in °
0.1671	0.2795	0.0000	181.4274
0.3010	0.2910	0.0000	127.1203
0.3719	0.3185	0.0000	280.7242
0.4514	0.3425	0.0000	309.4725
0.5685	0.3492	0.0000	50.8714
0.6844	0.3777	0.0000	31.8905
0.9382	0.3872	0.0000	219.9876
1.5140	0.4050	0.0000	263.8507
1.7286	0.4266	0.0000	47.4880
1.8690	0.4551	0.0000	209.2207
1.9849	0.4751	0.0000	154.7561
1.9282	0.4782	0.0000	308.3178
1.7279	0.5076	0.0000	325.3074
1.4645	0.5279	0.0000	341.6464
1.2380	0.5367	0.0000	166.3196
1.0503	0.5689	0.0000	122.1906
0.8788	0.5770	0.0000	353.4064
0.7205	0.6002	0.0000	93.1363
0.6153	0.6175	0.0000	290.5067
0.5773	0.6451	0.0000	137.8984
0.5419	0.6527	0.0000	166.7676
0.4809	0.6711	0.0000	219.3267
0.4187	0.6867	0.0000	182.2936
0.3658	0.7152	0.0000	254.9679
0.3329	0.7353	0.0000	64.6386
0.3099	0.7391	0.0000	145.2557
0.2943	0.7682	0.0000	107.9142
0.2843	0.7852	0.0000	61.5071
0.2771	0.8119	0.0000	1 96.3916
0.2697	0.8327	0.0000	290.5974
0.2588	0.8468	0.0000	24.4689
0.2457	0.8604	0.0000	203.1902
0.2330	0.8787	0.0000	34.8826
0.2207	0.8998	0.0000	142.3969
0.2089	0.9215	0.0000	347.0343
0.1977	0.9376	0.0000	219.7414
0.1870	0.9611	0.0000	57.3111
0.1776	0.9678	0.0000	355.3040
0.1728	0.9842	0.0000	83.2723
0.1742	1.0048	0.0000	48.9199